Angular-momentum structure of the yrast bands of deformed nuclei

S. Kahane* and S. Raman
Oak Ridge National Laboratory, Oak Ridge, Tennessee 37831

K. H. Bhatt
Department of Physics and Astronomy, University of Mississippi, University, Mississippi 38677
and Joint Institute for Heavy-Ion Research, Oak Ridge, Tennessee 37831

(Received 1 November 1996)

We have quantitatively analyzed the wave functions of the low-lying yrast states of deformed, heavy nuclei (specifically ^{238}U and ^{168}Er) given by different models to determine the relative contribution of the valence nucleons to the total angular momentum of the nucleus. In all models, an yrast state is generated, as expected, by collective contributions from both proton and neutron angular momenta. We have also examined the relative contribution of valence nucleons in the normal-parity states and in the abnormal-parity, high-j, intruder states to the yrast angular momentum. If the states with definite angular momenta projected from the Nilsson intrinsic state of the nucleus are assumed to provide a good approximation to the structure of the yrast band, the contribution of nucleons in the abnormal-parity states to the yrast angular momentum is shown to be about the same as that of nucleons in the normal-parity states. This result is in marked contrast to the assumption made in two prominent models (pseudo-SU_3 model and its symplectic extension and fermion dynamic symmetric model) that the nucleons in abnormal-parity states, do not, in the first approximation, contribute any angular momentum to the yrast band. We also find that the distribution of angular momenta contained in the intrinsic state of the abnormal-parity nucleons in the j^n configuration, which does not have any SU_3 symmetry, is surprisingly similar to the distribution of angular momenta contained in an SU_3 intrinsic state with the same average value of angular momentum. [S0556-2813(97)04706-7]

PACS number(s): 21.60.Fw, 21.60.Cs, 27.70.+q, 27.90.+b

I. INTRODUCTION

The simplest description of the yrast band of an axially symmetric deformed nucleus is provided by hydrodynamic or rigid-rotor models [1]. In these models, this band results from the rotation of a deformed intrinsic state (in its ground state) around an axis perpendicular to the axis of symmetry. Yrast states with increasing angular momenta $J=0,2,4,\ldots$ arise as a result of increasing kinetic energy of rotation. All nucleons participate in this collective rotation—although their actual motions would be different in the two models.

In shell models [2], low-lying states of nuclei are attributed to the dynamics of nucleons in a valence shell. Even though the majority of nucleons belong to a spherical core and remain dynamically inert, they still exert influence on the dynamics of valence nucleons by modifying the effective interactions and transition operators. In these models, the shortest route to a description of rotational states is provided by considering them to be a consequence of SU_3 symmetry based, one way or another, on the quadrupole-quadrupole (qq) interactions between (i) valence nucleons (pseudo-SU_3 model [3] and microscopic SU_3 model [4]) or (ii) s and d bosons representing nucleon pairs (interacting boson approximation [5]) or (iii) S and D nucleon pairs (fermion dynamic symmetry model [6]).

A more direct description of the yrast band of a deformed nucleus which does not necessarily invoke SU_3 symmetry is obtained by considering it to be the set of states of definite angular momenta projected from the lowest-energy intrinsic state [7]. The Nilsson model [8] provides a good approximation to this state. A Hartree-Fock (HF) calculation restricted to the valence configuration space [9] would provide an intrinsic state that is better, in principle, than the Nilsson state. Such calculations have been carried out and they confirm [10] that the Nilsson state is a good approximation to the intrinsic state of a heavy deformed nucleus.

In an earlier work [11] on the structure of the collective states in ^{56}Fe, a suggestion was made (by extension and inference) that the rotational features of heavy deformed nuclei could be a consequence of approximate macroscopic SU_3 symmetry even when a substantial number of nucleons have no microscopic SU_3 symmetry. This suggestion is pursued in this paper.

Exact diagonalization of the Hamiltonian matrices for different values of angular momenta in the chosen valence space have reproduced not only the rotationlike yrast bands but also many other low-lying states of light nuclei with nucleons in the $0p$ and $1s\,0d$ shells [12,13]. Such calculations have also been attempted for nuclei at the middle of the $1p\,0f$ shell [14]. This approach cannot be used, however, to describe the structure of heavy deformed nuclei because the configuration space is prohibitively large. However, a truncation scheme based on approximate quasi-SU_3 symmetry has been recently implemented [15] to describe rotational motion in the spherical shell model.

In general, the aim of nuclear models is to calculate those physical quantities for which measurements exist or can be made relatively easily. It turns out that models with significantly different internal content often produce numbers for measured quantities that are quite similar. Therefore, a mere

*Permanent address: Nuclear Research Center—Negev, Beer-Sheva, Israel.

listing of the agreement with the available measured quantities is insufficient to provide a proper appreciation of the inner workings of various models. A closer examination of the structure of the wave functions may provide a better understanding of the models and of the physics of the processes that these models are attempting to describe.

In this paper, we examine the structure of the yrast bands of highly deformed nuclei such as ^{238}U and ^{168}Er. We consider ^{208}Pb as the core for ^{238}U and ^{132}Sn as the core for ^{168}Er. Specifically, we want to determine the relative contributions of angular momenta J_π of valence protons (π) and J_ν of valence neutrons (ν) to the total angular momentum J of the yrast state. The states $|J_\pi\rangle$ and $|J_\nu\rangle$ have different microscopic structures in different nuclear models. However, the strong quadrupole correlation between these states—required to produce rotationally collective states—should be largely independent of their microscopic structure. We shall obtain a quantitative estimate of this correlation.

We also pay special attention to the role played by valence nucleons in the intruder abnormal-parity, high-j, single-particle (sp) states $0h_{11/2}$, $0i_{13/2}$, and $0j_{15/2}$ in the 50–82, 82–126, and 126–184 shells, respectively, in determining the angular-momentum structure of the yrast bands. Different models assign different (and sometimes contradictory) roles to nucleons in intruder levels. When these nucleons are allowed to participate in a unified collective motion, we want to know their contributions relative to those made by all other nucleons.

In Sec. II, we first describe the calculation of the probabilities of different J contained in a deformed intrinsic state denoted by $\mathcal{F}_K$. We then describe the structure of the projected state[1] $|JK\rangle$ in terms of states $|J_\pi K_\pi\rangle$ and $|J_\nu K_\nu\rangle$ projected from the proton and neutron parts of the intrinsic state. The state $|J_\pi K_\pi\rangle$ is further analyzed to determine the relative contribution of protons in the normal-parity (n) and abnormal-parity (a) states (with angular momenta $J_{\pi n}$ and $J_{\pi a}$, respectively) to the total J_π. A similar decomposition is done for the state $|J_\nu K_\nu\rangle$. This information is used to determine the probabilities that nucleons in n and a states (referred to loosely as n and a nucleons) contribute different angular momenta J_n and J_a to the total J of an yrast state.

In Sec. III, we consider the description of rotational states with models using SU_3 symmetry. In these models, the yrast states belong to the highest available SU_3 representation (abbreviated as rep) $[\lambda,\mu]$; that is, they can be projected from the most deformed intrinsic state of this rep. We describe the calculation of the probabilities of different angular momenta contained in this intrinsic state. States with total J resulting from the coupling of reps $[\lambda_\pi,\ \mu_\pi]$ of protons and $[\lambda_\nu,\ \mu_\nu]$ of neutrons are expanded in terms of the states $|[J_\pi\times J_\nu]J\rangle$.

In Secs. IV and V, we consider ^{238}U and ^{168}Er and outline their descriptions in terms of the pseudo-SU_3 model (PSM), interacting boson approximation (IBA), fermion dynamic symmetry model (FDSM), and single-shell asymptotic Nilsson model (SSANM). In their simplest implementations (and the ones currently available) the PSM and FDSM assume that nucleons in the intruder high-j state are coupled to angular momentum zero with *zero seniority*; the IBA and SSANM do not make this assumption. We examine the effect of this assumption on the structure of the yrast states of these nuclei by expanding $|J\rangle$ in terms of $|J_n\rangle$ and $|J_a\rangle$. In Sec. V C, we discuss briefly the microscopic SU_3 model and its treatment of the contributions of protons and neutrons in the n and a states to the total J of an yrast state of ^{168}Er.

The essential point of the description of rotational states in shell models using projected HF approaches or SU_3 symmetry is that the energy spectrum of yrast states results from differences in the energies (of states with different angular momenta) caused by the two-body interactions and *not* from the differences in the kinetic energies of rotation. This distinction is brought out in Sec. VI. Finally, a summary is given in Sec. VII.

II. DISTRIBUTION OF ANGULAR MOMENTA IN AN INTRINSIC STATE

In this section we describe the construction of an intrinsic state $\mathcal{F}_K$ and the procedure for projecting out various states with different angular momenta from this intrinsic state. We calculate the probability distributions of (i) total J contained in $\mathcal{F}_K$; (ii) J_π, in $\mathcal{F}^\pi_{K_\pi}$; (iii) J_ν, in $\mathcal{F}^\nu_{K_\nu}$; and (iv) J_π and J_ν, in the projected state $|J\rangle$. We then calculate the probabilities $P_3(J_\pi;J_{\pi n},J_{\pi a})$ that the state $|J_\pi\rangle$ projected from $|\mathcal{F}^\pi_{K_\pi}\rangle$ contains the states $|[J_{\pi n}\times J_{\pi a}]J_\pi\rangle$ and the corresponding probabilities $P_3(J_\nu;J_{\nu n},J_{\nu a})$ for neutrons. Finally, we calculate the probabilities $P_3(J;J_n,J_a)$ that the projected state $|J\rangle$ contains n and a nucleons coupled to J_n and J_a, respectively, and then the related probabilities $P_3(J;J_n,J_a=0)$.

A. Structure of the intrinsic state

Let $\phi^\alpha_k(x)$ be the deformed sp state of nucleons in an axially symmetric intrinsic state $\mathcal{F}_K(x)$. Here, $k=\langle j_{z'}\rangle$ is the projection of sp angular momentum along the symmetry axis (body-fixed z' axis), α labels different deformed sp states with same k value, and $K=\Sigma_i k_i$ (summed over all occupied states i) is the projection of the total angular momentum along the same axis. Generally, for an axially symmetric deformation, $K=0$ for even-even nuclei. Within the configuration space of a single major shell, $\phi^\alpha_k(x)$ can be expanded in terms of *spherical* sp states $\psi^j_k(x)$ as

$$\phi^\alpha_k(x)=\sum_j c^\alpha_{j,k}\psi^j_k(x). \tag{1}$$

For an intrinsic state symmetric about midplane, we have

$$c^\alpha_{j,-k}=(-)^{j-k}c^\alpha_{j,k}. \tag{2}$$

The simplest intrinsic state $\mathcal{F}_K$ is a Slater determinant constructed with occupied sp states ϕ^α_k. For example, consider an intrinsic state of four particles occupying states $\phi^{\alpha_i}_{k_i}$. This intrinsic state can be written as

[1]Occasionally, we refer to the projected states $|JK\rangle$, $|J_\pi K_\pi\rangle$, $|J_\nu K_\nu\rangle$, etc. more simply as $|J\rangle$, $|J_\pi\rangle$, $|J_\nu\rangle$, etc.

$$\mathcal{F}_K=\sqrt{\frac{1}{4!}}\begin{vmatrix}\phi_{k_1}^{\alpha_1}(1) & \phi_{k_2}^{\alpha_2}(1) & \phi_{k_3}^{\alpha_3}(1) & \phi_{k_4}^{\alpha_4}(1)\\ \phi_{k_1}^{\alpha_1}(2) & \cdots & \cdots & \phi_{k_4}^{\alpha_4}(2)\\ \phi_{k_1}^{\alpha_1}(3) & \cdots & \cdots & \phi_{k_4}^{\alpha_4}(3)\\ \phi_{k_1}^{\alpha_1}(4) & \phi_{k_2}^{\alpha_2}(4) & \phi_{k_3}^{\alpha_3}(4) & \phi_{k_4}^{\alpha_4}(4)\end{vmatrix}. \tag{3}$$

All intrinsic states appearing in this paper are of this type.

B. Projection of states with definite angular momenta from $\mathcal{F}_K$

The intrinsic state $\mathcal{F}_K$ is deformed and can be expanded in terms of the states $\Psi_K^{J'}$ with definite total angular momentum J' of valence nucleons as

$$\mathcal{F}_K(x)=\sum_{J'} C_{J'K}\Psi_K^{J'}(x), \tag{4}$$

where $\Psi_K^{J'}(x)\equiv\langle x|J'K\rangle$ are normalized wave functions of state $|J'K\rangle$. We want to determine the distribution $P_1(J)\equiv|C_{JK}|^2$ which gives the probability that $\mathcal{F}_K$ contains a state $|JK\rangle$ with definite J. This distribution is a partial measure of the correlation between different J states required to produce the intrinsic state. This correlation is produced by the mean field generated by the effective interactions in a chosen configuration space. Relative phases between different C_{JK} amplitudes, needed for specifying this correlation more completely, are omitted because they are not required in the current discussion.

Consider a projection operator $\mathcal{P}_K^J$, which, acting on an arbitrary intrinsic state, projects out the state $|JK\rangle$ with the wave function Ψ_K^J. Then, by definition

$$\mathcal{P}_K^J\mathcal{F}_K=\mathcal{P}_K^J\sum_{J'} C_{J'K}\Psi_K^{J'}=C_{JK}\Psi_K^J. \tag{5}$$

Therefore

$$\Psi_K^J=\frac{1}{C_{JK}}\mathcal{P}_K^J\mathcal{F}_K, \tag{6a}$$

$$\langle\Psi_K^J|\Psi_K^J\rangle=\frac{1}{C_{JK}^*C_{JK}}\langle\mathcal{F}_K|\mathcal{P}_K^J\mathcal{P}_K^J|\mathcal{F}_K\rangle=1. \tag{6b}$$

For any projection operator, $\mathcal{P}^2=\mathcal{P}$; hence,

$$|C_{JK}|^2=\langle\mathcal{F}_K|\mathcal{P}_K^J|\mathcal{F}_K\rangle. \tag{7}$$

The projection operator is given by [9]

$$\mathcal{P}_K^J=\frac{2J+1}{8\pi^2}\int (D_{KK}^J(\Omega))^*R(\Omega)d\Omega, \tag{8}$$

where $(D_{KK}^J(\Omega))$ are standard D functions [1] and $R(\Omega)=R(\alpha,\beta,\gamma)=e^{-i\alpha J_z}e^{-i\beta J_y}e^{-i\gamma J_z}$ is the rotation operator which rotates coordinates $\mathbf{x}$ to $\mathbf{x}'$ by the Euler angles $\Omega=\alpha,\beta,\gamma$. The integration is over all angles with $d\Omega=d\alpha\ \sin\beta\, d\beta\, d\gamma$.

We can write Eq. (7) as

$$|C_{JK}|^2=\frac{2J+1}{8\pi^2}\int (D_{KK}^J(\Omega))^*\langle\mathcal{F}_K|R(\Omega)|\mathcal{F}_K\rangle d\Omega. \tag{9}$$

The term $\langle\mathcal{F}_K|R(\Omega)|\mathcal{F}_K\rangle$ is just the overlap of $\mathcal{F}_K(x)$ with the same function rotated by the Euler angles Ω. If $\mathcal{F}_K$ is a determinant, we can write

$$\langle\mathcal{F}_K|R(\Omega)|\mathcal{F}_K\rangle=\langle\mathcal{F}_K|e^{-i\beta J_y}|\mathcal{F}_K\rangle=\det\,[N_{\sigma\tau}(\beta)]. \tag{10}$$

The $\sigma\tau$th element, $N_{\sigma\tau}(\beta)$, of this determinant is given by

$$N_{\sigma\tau}(\beta)=\sum_j c_{j,k_\sigma}^{\alpha_\sigma *}c_{j,k_\tau}^{\alpha_\tau}d_{k_\sigma k_\tau}^j(\beta), \tag{11}$$

where

$$d_{k_\sigma k_\tau}^j(\beta)=\langle jk_\sigma|e^{-i\beta J_y}|jk_\tau\rangle \tag{12}$$

and the c coefficients are defined in Eq. (1).

As an example, the $\sigma=2,\tau=3$ element $N_{23}(\beta)$ of $\det\,[N_{\sigma\tau}(\beta)]$ for the four-particle intrinsic state of Eq. (3) is given by

$$N_{23}(\beta)=\sum_j c_{j,k_2}^{\alpha_2 *}c_{j,k_3}^{\alpha_3}d_{k_2k_3}^j(\beta). \tag{13}$$

Once the sequence of occupied orbits ϕ_k^α in $\mathcal{F}_K$ is specified, $\det\,[N_{\sigma\tau}(\beta)]$ can be calculated. The probability $|C_{JK}|^2$ is obtained by evaluating Eq. (9). After carrying out the integration over the Euler angles α and γ, this equation reduces to

$$|C_{JK}|^2=\frac{2J+1}{2}\int d_{KK}^J(\beta)\langle\mathcal{F}_K|e^{-i\beta J_y}|\mathcal{F}_K\rangle\sin\beta\ d\beta. \tag{14}$$

Equation (14) is valid for a general intrinsic state, but here we shall calculate $|C_{JK}|^2$ only for determinant states of the type given by Eq. (3). The average value $\overline{J}$ of the total angular momentum contained in an intrinsic state $\mathcal{F}_K$ is defined by

$$\overline{J}=\sqrt{\langle J^2\rangle}, \tag{15}$$

where

$$\langle J^2\rangle=\sum_J J(J+1)|C_{JK}|^2 \tag{16}$$

is the average value of J^2 in $\mathcal{F}_K$.

C. Distribution of angular momenta of protons and neutrons in the projected state $|JK\rangle$

Because protons and neutrons share a common deformed mean field produced by effective interactions, their motions are correlated. A partial measure of this mean-field-generated π-ν correlations is given by the distribution $P_3(J;J_\pi,J_\nu)$, which denotes the probability that the yrast state $|J\rangle$ with total angular momentum J (projected from the intrinsic state

$\mathcal{F}_K$) contains protons and neutrons with corresponding angular momenta J_π and J_ν. This intrinsic state can be factored as

$$|\mathcal{F}_K\rangle = |\mathcal{F}^\pi_{K_\pi}\rangle |\mathcal{F}^\nu_{K_\nu}\rangle. \tag{17}$$

The states $|\mathcal{F}^\pi_{K_\pi}\rangle$ and $|\mathcal{F}^\nu_{K_\nu}\rangle$ can be expanded as

$$|\mathcal{F}^\pi_{K_\pi}\rangle = \sum_{J'_\pi} C^\pi_{J'_\pi K_\pi} |J'_\pi K_\pi\rangle \quad \text{and} \quad |\mathcal{F}^\nu_{K_\nu}\rangle = \sum_{J'_\nu} C^\nu_{J'_\nu K_\nu} |J'_\nu K_\nu\rangle, \tag{18}$$

where $|J'_\pi K_\pi\rangle$ and $|J'_\nu K_\nu\rangle$ are alternate notations for the wave functions $\Psi^{J'_\pi}_{K_\pi}$ and $\Psi^{J'_\nu}_{K_\nu}$, respectively. The squares of the expansion coefficients $|C^\pi_{J_\pi K_\pi}|^2$ and $|C^\nu_{J_\nu K_\nu}|^2$ can be calculated using Eq. (14) with $\mathcal{F}_K$ replaced by $\mathcal{F}^\pi_{K_\pi}$ or $\mathcal{F}^\nu_{K_\nu}$. Substituting Eq. (18) into Eq. (17), we obtain

$$\begin{aligned}\mathcal{F}_K &= \sum_{J'_\pi, J'_\nu} C^\pi_{J'_\pi K_\pi} C^\nu_{J'_\nu K_\nu} \Psi^{J'_\pi}_{K_\pi} \Psi^{J'_\nu}_{K_\nu} \\ &= \sum_{J'} \sum_{J'_\pi, J'_\nu} C^\pi_{J'_\pi K_\pi} C^\nu_{J'_\nu K_\nu} (J'_\pi J'_\nu K_\pi K_\nu | J'K) |[J'_\pi \times J'_\nu] J'K\rangle,\end{aligned} \tag{19}$$

where $(J'_\pi J'_\nu K_\pi K_\nu | J'K)$ are Clebsch-Gordan coefficients and $|[J'_\pi \times J'_\nu] J'K\rangle$ is the normalized and properly antisymmetrized state with total J' obtained by coupling J'_π and J'_ν. Comparing the expansions of $\mathcal{F}_K$ in Eqs. (19) and (4), we conclude that the wave function Ψ^J_K with a *specific* total J projected from $\mathcal{F}_K$ has the structure

$$\Psi^J_K = \frac{1}{C_{JK}} \sum_{J'_\pi, J'_\nu} C^\pi_{J'_\pi K_\pi} C^\nu_{J'_\nu K_\nu} (J'_\pi J'_\nu K_\pi K_\nu | JK) |[J'_\pi \times J'_\nu] JK\rangle. \tag{20}$$

This equation can be written as

$$\Psi^J_K = \sum_{J'_\pi, J'_\nu} A(J; J'_\pi, J'_\nu) |[J'_\pi \times J'_\nu] JK\rangle, \tag{21}$$

where

$$A(J; J'_\pi, J'_\nu) = \frac{C^\pi_{J'_\pi K_\pi} C^\nu_{J'_\nu K_\nu} (J'_\pi J'_\nu K_\pi K_\nu | JK)}{C_{JK}}. \tag{22}$$

The probability $P_3(J; J_\pi, J_\nu)$ that protons and neutrons contribute specific J_π and J_ν to the total J is given by

$$P_3(J; J_\pi, J_\nu) = |A(J; J_\pi, J_\nu)|^2. \tag{23}$$

These P_3 values satisfy the normalization condition

$$\sum_{J'_\pi, J'_\nu} P_3(J; J'_\pi, J'_\nu) \equiv \sum_{J'_\pi, J'_\nu} |A(J; J'_\pi, J'_\nu)|^2 = 1. \tag{24}$$

From Eqs. (24) and (22), we obtain

$$P_1(J) \equiv |C_{JK}|^2 = \sum_{J'_\pi, J'_\nu} |C^\pi_{J'_\pi K_\pi} C^\nu_{J'_\nu K_\nu} (J'_\pi J'_\nu K_\pi K_\nu | JK)|^2. \tag{25}$$

For axially symmetric even-even nuclei, all K values with subscripts appearing in the above formulas are zero in addition to $K=0$. Various probabilities for the yrast states of ^{238}U and ^{168}Er will be examined in Secs. IV and V, respectively.

D. Distribution of proton and neutron angular momenta in *n* and *a* states

Let $N_{\pi n}$ and $N_{\pi a}$ represent valence protons in n and a states, respectively. Then $N_\pi = N_{\pi n} + N_{\pi a}$ is the total number of valence protons. Similarly, we write $N_\nu = N_{\nu n} + N_{\nu a}$ for valence neutrons. If n and a protons share a common field, their $J_{\pi n}$ and $J_{\pi a}$ must be correlated in a specific way to generate the states $|J_\pi\rangle$. We are interested in the probabilities $P_3(J_\pi; J_{\pi n}, J_{\pi a})$ and the related probabilities $P_3(J_\nu; J_{\nu n}, J_{\nu a})$ and $P_3(J; J_n, J_a)$. They provide partial measures of the quadrupole correlations between the n and a protons, n and a neutrons, and n and a nucleons, respectively.

In general, the proton intrinsic state can be factored as

$$\mathcal{F}^\pi_{K_\pi} = \mathcal{A}\, \mathcal{F}^{\pi n}_{K_{\pi n}} \mathcal{F}^{\pi a}_{K_{\pi a}}, \tag{26}$$

where $\mathcal{A}$ implies antisymmetrization between the n and a protons. Because the n and a sp states are different, this antisymmetrization puts no restriction on the angular-momentum content of $\mathcal{F}^\pi_{K_\pi}$. Analogous to Eq. (23), we obtain

$$P_3(J_\pi; J_{\pi n}, J_{\pi a}) = \frac{|C^\pi_{J_{\pi n} K_{\pi n}} C^\pi_{J_{\pi a} K_{\pi a}} (J_{\pi n} J_{\pi a} K_{\pi n} K_{\pi a} | J_\pi K_\pi)|^2}{|C_{J_\pi K_\pi}|^2}. \tag{27}$$

Analogous to Eq. (25), we also obtain

$$P_1(J_\pi) = \sum_{J'_{\pi n}, J'_{\pi a}} |C^\pi_{J'_{\pi n} K_{\pi n}} C^\pi_{J'_{\pi a} K_{\pi a}} (J'_{\pi n} J'_{\pi a} K_{\pi n} K_{\pi a} | J_\pi K_\pi)|^2. \tag{28}$$

Similar expressions hold for neutrons.

E. Distribution of total angular momentum in *n* and *a* states

The states $|J\rangle$ are generated by n-a correlations in a way completely analogous to π-ν correlations. Following again the procedures used to derive Eqs. (23) and (27), we get

$$P_3(J; J_n, J_a) = \frac{|C^n_{J_n K_n} C^a_{J_a K_a} (J_n J_a K_n K_a | JK)|^2}{|C_{JK}|^2}, \tag{29}$$

where

$$|C^n_{J_n K_n}|^2 = \sum_{J'_{\pi n}, J'_{\nu n}} \left| C^\pi_{J'_{\pi n} K_{\pi n}} C^\nu_{J'_{\nu n} K_{\nu n}} (J'_{\pi n} J'_{\nu n} K_{\pi n} K_{\nu n} | J_n K_n) \right|^2. \tag{30}$$

A similar expression holds for $|C^{a}_{J_aK_a}|^2$. The contribution of a given J_a to the total J irrespective of the J_n values is given by

$$P_2(J;J_a)=\sum_{J_n} P_3(J;J_n,J_a). \tag{31}$$

One of our aims is to obtain the probabilities that the state $|J\rangle$ has a component with $J_a=0$ in which the a neutrons and a protons are separately coupled to angular momentum zero (as assumed in PSM and FDSM). These joint probabilities are given by

$$P_5[J;J_n,J_a=0\,(J_{\pi a}=J_{\nu a}=0)] = P_3(J;J_n,J_a=0)\times P_3(J_a=0;J_{\pi a}=0,J_{\nu a}=0). \tag{32}$$

III. ANGULAR MOMENTA CONTAINED IN THE INTRINSIC STATES OF SU_3-SYMMETRY MODELS

The yrast band of states with definite J contained in a SU_3 rep $[\lambda,\mu]$ can be projected from the highest-weight intrinsic state $\mathcal{F}[\lambda,\mu]$. For prolate nuclei of interest to us here, $\lambda > \mu$. An intrinsic state with $\mu\neq 0$ is triaxial in shape and contains different K bands with $K=\mu,\mu-2,\ldots,1$ or 0. A band with $K=0$ contains states Ψ^J_K with $J=0,2,4,\ldots,\lambda+\mu$. Bands with $K\neq 0$ contain $J=K,K+1,\ldots,K+\lambda$ states. The states Ψ^J_K can be obtained from $\mathcal{F}[\lambda,\mu]$ by the Elliott projection procedure [16,17]. The angular-momentum content of the $\mathcal{F}[\lambda,\mu]$ state can be brought out by expanding it in terms of states $\Psi([\lambda,\mu]JK)$ as

$$\mathcal{F}[\lambda,\mu]=\sum_{J',K'} a([\lambda,\mu];J',K')\Psi([\lambda,\mu]J'K'). \tag{33}$$

Projected states $\Psi([\lambda,\mu]JK)$ of the same J belonging to different K bands are not orthogonal. The overlap between two such states is given by

$$\langle\Psi([\lambda,\mu]JK)|\Psi([\lambda,\mu]JK')\rangle = \frac{\mathcal{R}([\lambda,\mu]JKK')}{a([\lambda,\mu];J,K)a([\lambda,\mu];J,K')}. \tag{34}$$

Because the state $|\Psi([\lambda,\mu]JK\rangle$ is normalized, we get

$$|a([\lambda,\mu];J,K)|^2=\mathcal{R}([\lambda,\mu]JKK). \tag{35}$$

The functions[2] $\mathcal{R}([\lambda,\mu]JKK')$ derived by Elliott [16,17] are given by

$$\mathcal{R}([\lambda,\mu]JKK')=\frac{(2J+1)\mu!}{8\pi^2}\sum_{n=0}^{\mu}\frac{(-)^n}{n!(\mu-n)!}\,I_\alpha\,I_\gamma\,I_\beta, \tag{36}$$

where

$$I_\alpha=\int_0^{2\pi} d\alpha\; e^{iK'\alpha}\sin(\alpha)^n\cos(\alpha)^{\mu-n}, \tag{37a}$$

$$I_\gamma=\int_0^{2\pi} d\gamma\; e^{iK\gamma}\sin(\gamma)^n\cos(\gamma)^{\mu-n}, \tag{37b}$$

$$I_\beta=\int_0^{\pi}\sin\beta\; d\beta\; d^J_{K'K}(\beta)\cos(\beta)^{n+\lambda}. \tag{37c}$$

Convenient algebraic formulas for calculating $\mathcal{R}([\lambda,\mu]JKK'=K)$ have been provided by Vergados [18] up to $\mu=4$.

The normalization of $\mathcal{F}[\lambda,\mu]$ given in Eq. (33) together with Eq. (34) gives the normalization condition on the $\mathcal{R}$ function

$$\langle\mathcal{F}[\lambda,\mu]|\mathcal{F}[\lambda,\mu]\rangle=\sum_J\sum_{K'}\sum_K \mathcal{R}([\lambda,\nu]JKK')=1. \tag{38}$$

For axially symmetric reps $[\lambda,0]$, $K=K'=0$. In this case, we get

$$\sum_J \mathcal{R}([\lambda,\nu]J,K=0,K'=0)=\sum_J |a([\lambda,0];J,0)|^2=1, \tag{39}$$

and $|a([\lambda,0];J,0)|^2$ is the probability $P_1(SU_3[\lambda,\mu]:J)$ that the intrinsic state $\mathcal{F}[\lambda,0]$ contains angular momentum J.

For triaxial reps $[\lambda,\mu]$, we shall associate the yrast band with only the $K=0$ band. In this case, the sum $\Sigma_J|a([\lambda,\mu];J,K=0)|^2<1$. We can multiply the amplitudes $a([\lambda,\mu];J,K=0)$ by a normalization constant N_0 such that $N_0^2\Sigma_J|a([\lambda,\mu];J,K=0)|^2=1$. We regard $N_0^2\,|a([\lambda,\mu];J,K=0)|^2$ as the probability $P_1(SU_3\;[\lambda,\mu]:J,K=0)$ that the $K=0$ band contains angular momentum J.

In the following sections, we shall use the results of this section to calculate the distributions of $J_{\pi n}$, $J_{\pi a}$, $J_{\nu n}$, $J_{\nu a}$, J_π, J_ν, J_n, J_a, and J in the Nilsson or SU_3 intrinsic states for ^{238}U (Sec. IV) and ^{168}Er (Sec. V). The Nilsson intrinsic states are axially symmetric in both cases while the SU_3 reps are axially symmetric in the ^{238}U case and either axially symmetric or triaxial in the ^{168}Er case depending on the distribution of neutrons in n and a states.

IV. STRUCTURE OF THE YRAST BAND OF $^{238}_{92}U_{146}$

The highest angular momentum of the yrast band observed experimentally in ^{238}U till now is $J_{max}=30$ [19]. In a shell-model description, this band arises as a result of interactions among valence nucleons. With $^{208}_{82}Pb_{126}$ as the core, the ten valence protons in $^{238}_{92}U_{146}$ are confined to the sp (notation $n\not{l}j$) states $(0h_{9/2},\ 1f_{7/2})$, $(1f_{5/2},\ 2p_{3/2})$, $2p_{1/2}$, and to the high-spin intruder state $0i_{13/2}$ appropriate for the 82–126 major shell. The 20 valence neutrons occupy the $(0i_{11/2},\ 1g_{9/2})$, $(1g_{7/2},\ 2d_{5/2})$, $(2d_{3/2},\ 3s_{1/2})$ states and the intruder $0j_{15/2}$ state in the 126–184 shell.

[2]We use the notation $\mathcal{R}([\lambda,\mu]JKK')$ in place of the usual notation $P([\lambda,\mu]JKK')$ to avoid confusion with probabilities denoted by P.

A. Pseudo-SU_3 model (PSM)

In the PSM, doublets of sp states of normal parity (those within parentheses in the preceding paragraph) are considered to be pseudospin doublets attributed to pseudoangular momenta $\tilde{l}_\pi = 4$, 2, and 0 forming a $\tilde{N} = 4$ pseudo-oscillator shell and to $\tilde{l}_\nu = 5$, 3, and 1 forming a $\tilde{N} = 5$ shell. The observed near degeneracy of these doublets (implying small pseudo-spin-orbit coupling) together with the dominance of the qq component of the effective interaction has led to the introduction of an approximately conserved pseudo-SU_3 symmetry within the n sector of configuration space [3]. The coupling of a nucleons can, in principle, lead to a breakdown of SU_3 symmetry for the n nucleons. The symmetry is, however, preserved if one assumes (for simplicity) that the a nucleons remain coupled to zero seniority. With this assumption, PSM identifies the yrast band as belonging to the highest SU_3 rep of nucleons occupying the n states.

In the case of $^{238}_{92}U_{146}$, the number of particles occupying n and a states are determined from the Nilsson energy-level diagram at the measured deformation of $\beta \approx 0.25$. These numbers are $N_n^\pi = 6$, $N_a^\pi = 4$, $N_n^\nu = 12$, and $N_a^\nu = 8$. The total numbers of nucleons in these two groups are $N_n = 18$ and $N_a = 12$. These numbers are assumed to be conserved in the dynamics of PSM implemented thus far.

The assumptions made in the simplest and extensively implemented calculations in the PSM (and in FDSM) regarding the structure of the yrast bands of nuclei imply certain restrictions on the relative importance of different parts of the pairing interaction. For example, transitions of the type $j_{1n}j_{2n} \rightleftharpoons j_{1a}j_{2a}$ for proton or neutron pairs are an important consequence of the pairing interaction. Such transitions connecting n and a sectors are suppressed, for the sake of simplicity, with the assumption that the yrast band can be well described with constant values of N_n and N_a. Transitions of the type $j_{1n}j_{2n} \rightleftharpoons j'_{1n}j'_{2n}$ within the n sector also form an important part of the pairing interaction. Again, the simplifying assumption made in the PSM that the yrast band is well described by a *single* SU_3 rep implies that pairing may also be neglected in the n sector in comparison with the qq interaction. The remaining part of the pairing interaction acts only within the a sector. It must be abnormally strong to maintain the a nucleons in seniority-zero states in the deformed mean field of the nucleus. Although this conclusion is inevitable, an explicit pairing interaction for the a nucleons is not used in the PSM or FDSM to produce the quasi spherical band—with the maximally deformed n nucleons coupled to the seniority-zero state of the a nucleons—as the yrast band. In these models, such a band is made yrast more easily by just assuming it to be the lowest-energy state. This assumption is justified by the success of these models in reproducing the experimental data.

1. Angular-momentum content of valence protons and neutrons

The highest pseudo-SU_3 rep of 6 protons in the $\tilde{N} = 4$ shell is $\pi[18,0]$ and of 12 neutrons in the $\tilde{N} = 5$ shell is $\nu[36,0]$ (see Table 8 of Ref. [20]). The $\pi[18,0]$ rep contains states with $J_\pi = 0,\ 2,\ 4, \ldots, 18$, and the $\nu[36,0]$ rep states with $J_\nu = 0,\ 2,\ 4, \ldots, 36$. The yrast band of ^{238}U is described by the highest SU_3 rep $[54,0]$ obtained by coupling the $\pi[18,0]$ and $\nu[36,0]$ reps. This band, therefore, extends up to the $J_{\max} = (J_n)_{\max} = 54$ state.

We want to examine the structure of the yrast state $|J\rangle$ in terms of states $|J_{\pi n}\rangle$ and $|J_{\nu n}\rangle$. To do so, we use the Elliott expansion [Eq. (33)] of $\mathcal{F}^\pi[\lambda_\pi, \mu_\pi]$ and $\mathcal{F}^\nu[\lambda_\nu, \mu_\nu]$ in terms of the states $\Psi^\pi([\lambda_\pi, \mu_\pi] J_\pi K_\pi)$ and $\Psi^\nu([\lambda_\nu, \mu_\nu] J_\nu K_\nu)$, respectively, belonging to different K_π and K_ν bands. For ^{238}U, $\mu = 0$ for both protons and neutrons. Therefore, $K_\pi = K_\nu = 0$. We expand [cf. Eq. (33) with the expansion coefficient a replaced by u^π, u^ν, and U]:

$$\mathcal{F}_n^\pi(\mathrm{PSM}[18,0]) = \sum_{J'_{\pi n}} u^\pi([18,0]; J'_{\pi n}, 0)\Psi^\pi([18,0] J'_{\pi n} 0), \quad J'_{\pi n} = 0,2, \ldots, 18, \tag{40a}$$

$$\mathcal{F}_n^\nu(\mathrm{PSM}[36,0]) = \sum_{J'_{\nu n}} u^\nu([36,0]; J'_{\nu n}, 0)\Psi^\nu([36,0] J'_{\nu n} 0), \quad J'_{\nu n} = 0,2, \ldots, 36, \tag{40b}$$

$$\mathcal{F}_n(\mathrm{PSM}[54,0]) = \sum_{J'_n} U([54,0]; J'_n, 0)\Psi([54,0] J'_n 0), \quad J'_n = 0,2, \ldots, 54. \tag{40c}$$

For later convenience, these equations are written in a simpler notation as

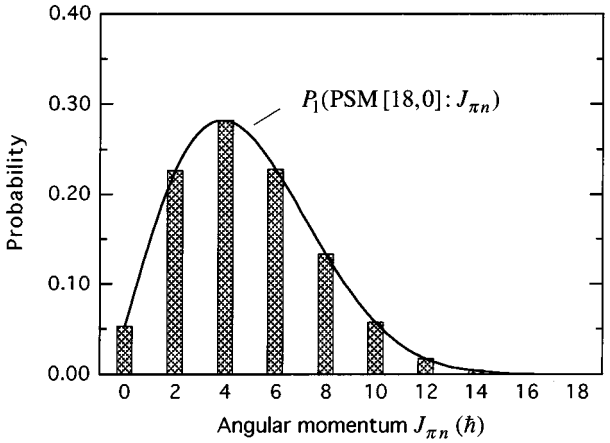

FIG. 1. Probability distribution P_1 that the PSM SU_3 [18,0] intrinsic state contains a state with definite angular momentum $J_{\pi n}$. The smooth curve represents what is actually a distribution restricted to even values of $J_{\pi n}$. Hereafter all P_1 distributions are shown as smooth curves. The curve shown here is again reproduced in Fig. 2(a).

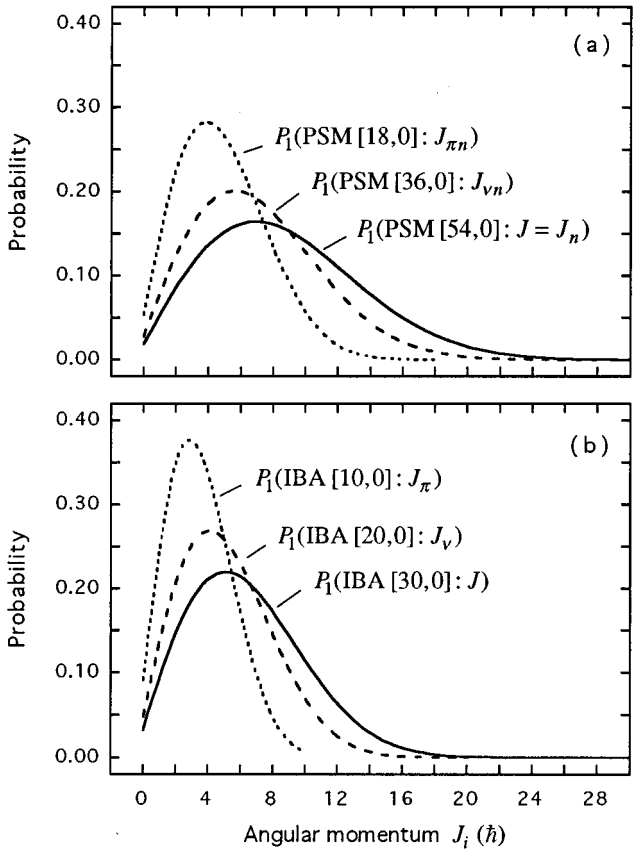

FIG. 2. (a) P_1 distributions as a function of J_i. Depending on the curve, the abscissa is $J_{\pi n}$, $J_{\nu n}$, or J in (a) and J_π, J_ν, or J in (b). The stated PSM and IBA SU_3 representations are for ^{238}U.

$$\mathcal{F}_n^{\pi}(\mathrm{PSM}[18,0]) = \sum_{J'_{\pi n}} u^{\pi n}_{J'_{\pi n}} |J'_{\pi n}\rangle, \tag{41a}$$

$$\mathcal{F}_n^{\nu}(\mathrm{PSM}[36,0]) = \sum_{J'_{\nu n}} u^{\nu n}_{J'_{\nu n}} |J'_{\nu n}\rangle, \tag{41b}$$

$$\mathcal{F}_n(\mathrm{PSM}[54,0]) = \sum_{J'_n} U^{n}_{J'_n} |J'_n\rangle. \tag{41c}$$

Quantities $|u^{\pi}([18,0];J_{\pi n},0)|^2$ and $|u^{\nu}([36,0];J_{\nu n},0)|^2$ give the probabilities $P_1(\mathrm{PSM}[18,0]:J_{\pi n})$ and $P_1(\mathrm{PSM}[36,0]:J_{\nu n})$ that the intrinsic states in $\pi[18,0]$ and $\nu[36,0]$ reps contain $J_{\pi n}$ and $J_{\nu n}$, respectively. These probabilities are evaluated using Eqs. (35) and (36) and plotted in Figs. 1 and 2(a). The average angular momenta $\overline{J_{\pi n}}$ and $\overline{J_{\nu n}}$ in these SU_3 states are 6.0 and 8.5, respectively. The quantity $|U([54,0];J,0|^2$ gives the probability $P_1(\mathrm{PSM}[54,0]:J)$ that the intrinsic state of nucleons in n states contains a state of the yrast band with angular momentum J; this probability is also shown in Fig. 2(a). The average angular momentum in the [54,0] rep is $\overline{J} = 10.4$.

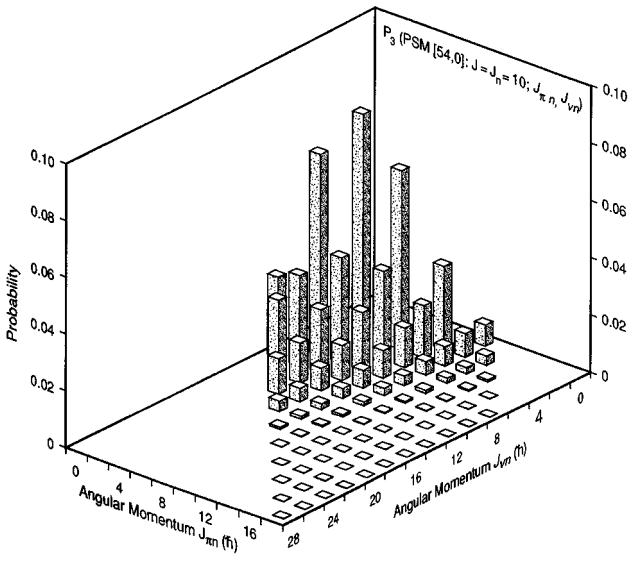

FIG. 3. A three-dimensional view of the P_3 distribution that the yrast state $|J\rangle$ with $J=10$ in ^{238}U contains the state $|[J_{\pi n}\times J_{\nu n}]J\rangle$ according to PSM.

2. Collectivity of the distribution of $J_{\pi n}$ and $J_{\nu n}$ in states $|J_n\rangle$

We can use the projection procedure described in Sec. II to show [cf. Eq. (20)] that the state $\Psi([54,0]J_n0)$ can be written in terms of $J_{\pi n}$ and $J_{\nu n}$ as

$$\Psi([54,0]J_n0) \equiv |\mathrm{PSM}{:}J_n\rangle = \sum_{J'_{\pi n},J'_{\nu n}} A(\mathrm{PSM}{:}J_n;J'_{\pi n},J'_{\nu n}) \times |[J'_{\pi n}\times J'_{\nu n}]J_n\rangle, \tag{42}$$

where

$$|A(\mathrm{PSM}{:}J_n;J'_{\pi n},J'_{\nu n})|^2 = \frac{|u^{\pi}([18,0];J'_{\pi n},0)\ u^{\nu}([36,0];J'_{\nu n},0)(J'_{\pi n}J'_{\nu n}00|J0)|^2}{|U([54,0];J,0)|^2} \tag{43}$$

is the probability $P_3(\mathrm{PSM}{:}J_n;J'_{\pi n},J'_{\nu n})$ that $|J_n\rangle$ contains the state $|[J'_{\pi n}\times J'_{\nu n}]J_n\rangle$. The P_3 distributions of $J_{\pi n}$ and $J_{\nu n}$ in the yrast state with total $J=J_n=10$ is shown as a three-dimensional plot in Fig. 3. These distributions for other J states are also three-dimensional but they are shown in Figs. 4(a)–4(d) for the $J=J_n=0$, 2, 4, and 6 states as two-dimensional plots to convey more quantitatively the fragmentation of an yrast state $|J\rangle$ into components of the type $|[J_{\pi n}\times J_{\nu n}]J_n\rangle$. Each state $|J\rangle$ has significant contributions from many of the possible couplings of the angular momenta of n protons and n neutrons which share the common deformed field. The probability that any J is generated by neutrons acting alone ($J_{\pi n}=0, J_{\nu n}=J$) or by protons acting alone ($J_{\pi n}=J, J_{\nu n}=0$) is small (only $\sim$7%). The n protons and n neutrons contribute collectively to the total J.

The contribution of a given $J_{\pi n}$ irrespective of the $J_{\nu n}$ values is given by [cf. Eq. (31)]

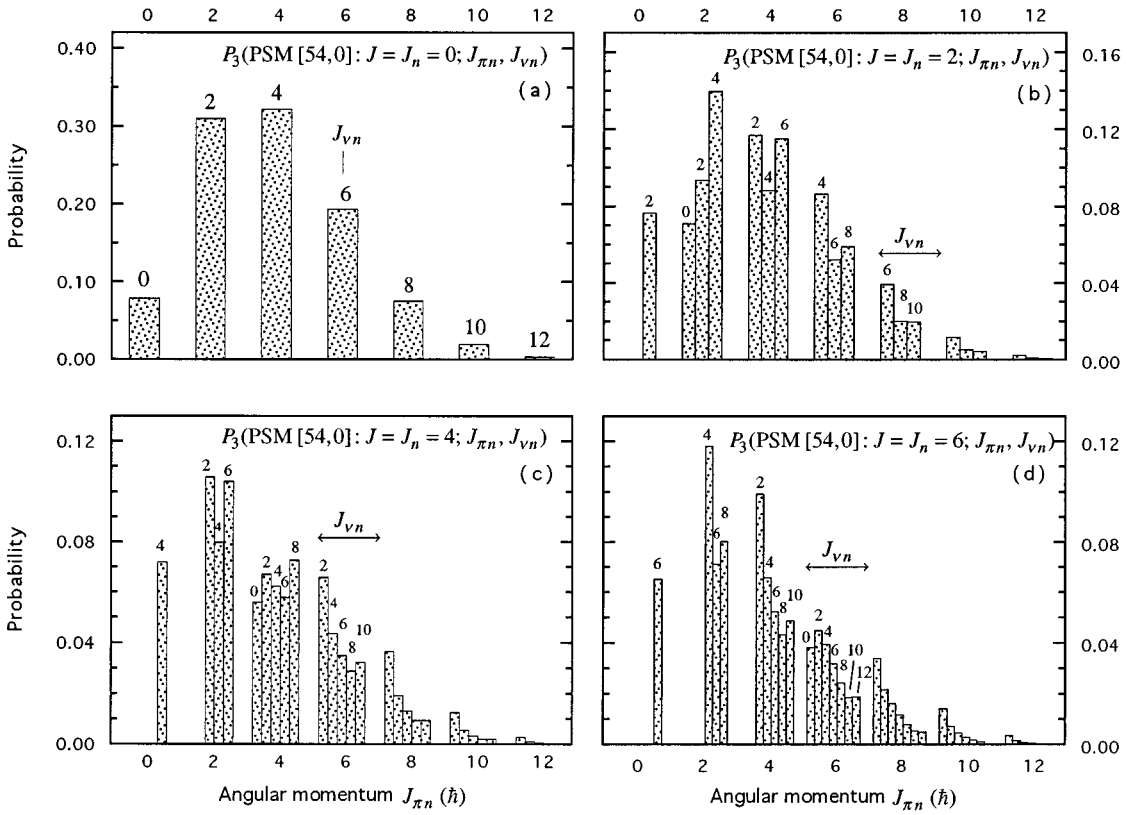

FIG. 4. Probability distribution P_3 that a particular yrast state $|J\rangle$ in ^{238}U contains the state $|[J_{\pi n}\times J_{\nu n}]J\rangle$ according to PSM.

$$P_2(J=J_n;J_{\pi n})=\sum_{J'_{\nu n}} P_3(J=J_n;J_{\pi n},J'_{\nu n}). \tag{44}$$

The $P_2(\text{PSM:}J=J_n;J_{\pi n})$ distributions are shown in Fig. 5(a). They are surprisingly similar regardless of J.

3. Distribution of J_n and J_a in states $|J\rangle$

According to PSM assumptions, $\Psi_J=\Psi_{n(J_n)}\Psi_{a(J_a=0)}$, and the probability that the total J results from the coupling of J_n and $(J_a=0)$ is given by

$$P_3(\text{PSM:}J;J_n,J_a=0)=1 \quad \text{for} \quad J=J_n, \tag{45a}$$

$$=0 \quad \text{otherwise.} \tag{45b}$$

Figure 6 illustrates the effect of this assumption made in PSM. The reason for the qualitative difference between $P_3(\text{PSM:}J;J_n,J_a)$ in Fig. 6 and $P_3(\text{PSM:}J;J_{\pi n},J_{\nu n})$ in Fig. 4 is that in PSM the seniority-zero assumption for a nucleons quenches the mean-field-induced correlations between the n and a nucleons.

4. Relation between measured electric quadrupole moment and $(J_\pi)_{max}$

The mass quadrupole moment of Q_π of the a-proton intrinsic state belonging to an SU_3 rep $[\lambda_\pi,0]$ is $Q_\pi=2\lambda_\pi=2(J_\pi)_{\max}$ in units of the oscillator parameter $\alpha^2=\hbar/(M\omega)=0.0101A^{1/3}$ b. Here $(J_\pi)_{\max}$ is the maximum angular momentum contained in the rep $[\lambda_\pi,0]$. The measured electric quadrupole moment Q_0 has contributions from both valence protons and core protons (the latter polarized by valence nucleons). A rough estimate by Mottelson [21] shows that core protons contribute about half of the intrinsic electric quadrupole moment. Hence the contribution of valence (v) protons to the intrinsic electric moment is $Q^v_{0,\pi}\approx\frac{1}{2}Q_0$. The measured intrinsic quadrupole moment of ^{238}U is $Q_0=11.0\ e$ b$=176\ e\alpha^2$ [22] and hence $Q^v_{0,\pi}\approx 88\ e\alpha^2$. The implied mass quadrupole moment of valence protons is $Q^v_\pi\approx 88\ \alpha^2$. If valence protons belonged to an SU_3 rep $[\lambda^*_\pi,0]$, the intrinsic mass quadrupole moment would be $Q^v_\pi=2\lambda^*_\pi$. Equating these two values, we obtain $\lambda^*_\pi=44$. The SU_3 rep $\pi[44,0]$ and $(J_\pi)_{\max}=44$ implied for valence protons by the measured intrinsic quadrupole moment are significantly larger than the PSM rep $\pi n[18,0]$ and $(J_{\pi n})_{\max}=18$ of only the n protons.

B. Interacting boson approximation (IBA)

In IBA-2, the 10 valence protons of $^{238}_{92}\text{U}_{146}$ are represented by 5 π bosons and the 20 valence neutrons by 10 ν bosons. In the SU_3 limit, the boson reps are $\pi[10,0]$ and $\nu[20,0]$, and the yrast band is described by $[30,0]$. These reps are significantly smaller than the corresponding ones in PSM. The intrinsic states can be expanded as [cf. Eq. (41)]

$$\mathcal{F}^\pi(\text{IBA}[10,0])=\sum_{J'_\pi} v^\pi_{J'_\pi}|J'_\pi\rangle, \quad J'_\pi=0,2,\ldots,10, \tag{46a}$$

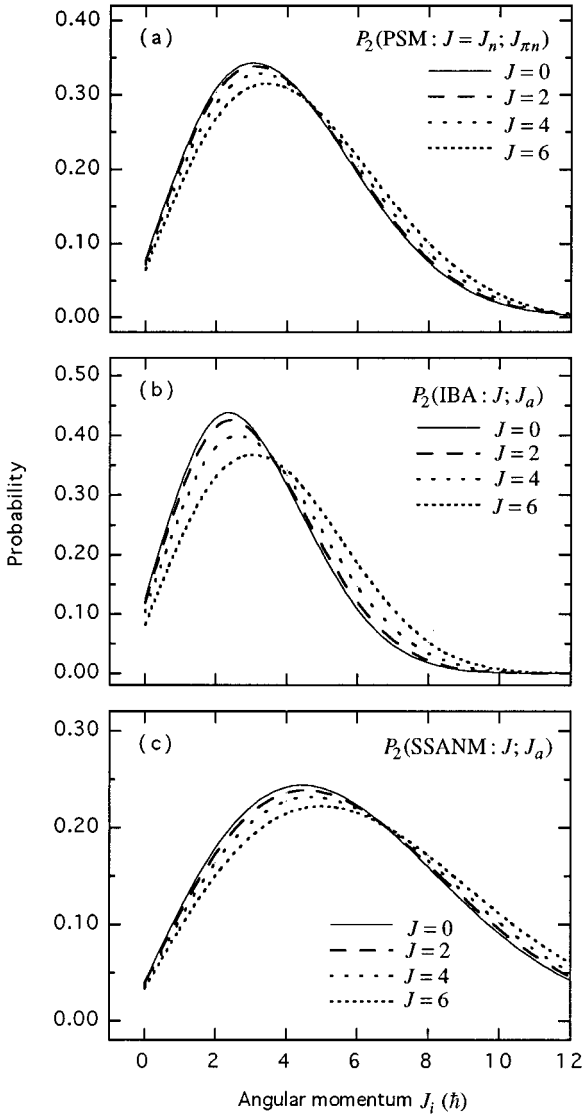

FIG. 5. Probability distributions P_2 as a function of J_i. The abscissa is $J_{\pi n}$ in (a), J_a in (b), and J_a in (c). These results are for ^{238}U.

$$\mathcal{F}^{\nu}(\mathrm{IBA}[20,0]) = \sum_{J'_\nu} v^{\nu}_{J'_\nu} |J'_\nu\rangle, \quad J'_\nu = 0,2,\ldots,20, \tag{46b}$$

$$\mathcal{F}(\mathrm{IBA}[30,0]) = \sum_{J'} V_{J'} |J'\rangle, \quad J' = 0,2,\ldots,30. \tag{46c}$$

The distributions $P_1(\mathrm{IBA}[10,0]{:}J_\pi)$, $P_1(\mathrm{IBA}[20,0]{:}J_\nu)$, and $P_1(\mathrm{IBA}[30,0]{:}J)$ are plotted in Fig. 2(b).

1. Introducing n and a bosons in IBA-2

Even though it would violate the spirit of IBA to distinguish between bosons in n and a states, we do so for comparing the structure of the yrast states in IBA-2 with those in PSM and FDSM. In IBA-2, s and d bosons are supposed to represent the lowest quadrupole collective states of two identical nucleons with $J=0$ and $J=2$, respectively, in the valence sp space. Both n and a sp states contribute to these coherent pair states. If we were to distinguish between n and a bosons, the n bosons (s_n, d_n) would represent the n-nucleon pair states, and the a bosons (s_a, d_a) the a-nucleon pair states. To mimic PSM, we assume that the numbers N_n of n bosons and N_a of a bosons remain separately constant, whereas in IBA-2 only the total number of bosons, $N = N_n + N_a$, would remain constant.

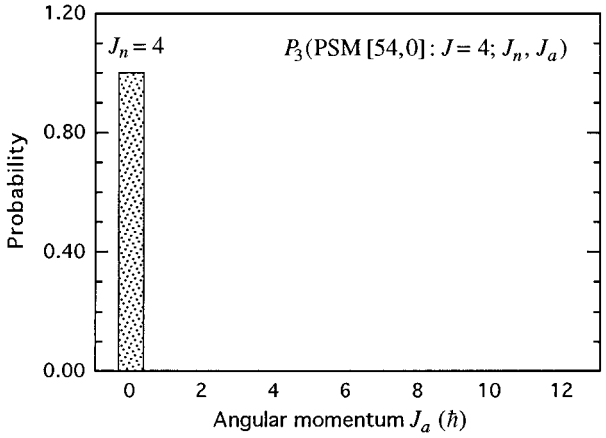

FIG. 6. Probability distribution P_3 that a particular yrast state $|J\rangle$ with $J = J_n = 4$ contains the state $|[J_n \times J_a]J\rangle$ according to PSM. The P_3 distribution for any other J $(=J_n)$ up to $J_{\max}=54$ is the same as that shown here for $J=4$. These results are for ^{238}U.

In ^{238}U, there are three π bosons of the n type and two of the a type. The corresponding SU_3 reps are $\pi n[6,0]$ and $\pi a[4,0]$. Similarly, the ν-boson reps are $\nu n[12,0]$ and $\nu a[8,0]$. The highest SU_3 reps of n and a nucleons are, therefore, $n[18,0]$ and $a[12,0]$.

2. Comparison of the π-ν distributions in PSM and IBA-2 within the n sector

The intrinsic states $\mathcal{F}^{\pi n}$, $\mathcal{F}^{\nu n}$, and $\mathcal{F}^{n}$ are expanded as

$$\mathcal{F}^{\pi n}(\mathrm{IBA}[6,0]) = \sum_{J'_{\pi n}} v^{\pi n}_{J'_{\pi n}} |J'_{\pi n}\rangle, \quad J'_{\pi n} = 0,2,\ldots,6, \tag{47a}$$

$$\mathcal{F}^{\nu n}(\mathrm{IBA}[12,0]) = \sum_{J'_{\nu n}} v^{\nu n}_{J'_{\nu n}} |J'_{\nu n}\rangle, \quad J'_{\nu n} = 0,2,\ldots,12, \tag{47b}$$

$$\mathcal{F}^{n}(\mathrm{IBA}[18,0]) = \sum_{J'_n} V^{n}_{J'_n} |J'_n\rangle, \quad J'_n = 0,2,\ldots,18, \tag{47c}$$

where the coefficients $v^{\pi n}_{J'_{\pi n}}$, $v^{\nu n}_{J'_{\nu n}}$, and $V^{n}_{J'_n}$ are determined from Eqs. (35) and (36). The states $|J'_n\rangle$ of n bosons are given by

$$|\mathrm{IBA}{:}J_n\rangle = \sum_{J'_{\pi n}, J'_{\nu n}} A(\mathrm{IBA}{:}J_n; J'_{\pi n}, J'_{\nu n}) |[J'_{\pi n} \times J'_{\nu n}]J_n\rangle, \tag{48}$$

where

$$P_3(\text{IBA:}J_n;J'_{\pi n},J'_{\nu n}) \equiv |A(\text{IBA:}J_n;J'_{\pi n},J'_{\nu n})|^2 = \frac{|v^{\pi n}_{J'_{\pi n}} v^{\nu n}_{J'_{\nu n}} (J'_{\pi n} J'_{\nu n} 00|J_n 0)|^2}{|V^n_{J_n}|^2} \tag{49}$$

is the probability that J_n contains the state $|[J'_{\pi n}\times J'_{\nu n}]J_n\rangle$.

The IBA rep [18,0] for n bosons is significantly smaller than the PSM rep [54,0] for n nucleons. Hence, details of the distributions of J_n over $J_{\pi n}$ and $J_{\nu n}$ would be different in these two models, but the overall distributions should be qualitatively similar because of SU_3 symmetry. A quantitative measure of this similarity can be obtained by calculating the overlap between the states $|\,\text{IBA:}J_n\rangle$ and $|\text{PSM:}J_n\rangle$ given by Eqs. (48) and (42), respectively, which are both expressed in terms of the components $|[J_{\pi n}\times J_{\nu n}]J_n\rangle$. This overlap is given by

$$\langle \text{IBA:}J_n|\text{PSM:}J_n\rangle = \sum_{J'_{\pi n},J'_{\nu n}} [A(\text{IBA:}J_n;J'_{\pi n},J'_{\nu n})][A(\text{PSM:}J_n;J'_{\pi n},J'_{\nu n})] \times \langle \text{IBA}[J'_{\pi n}\times J'_{\nu n}]J_n \mid \text{PSM}[J'_{\pi n}\times J'_{\nu n}]J_n\rangle. \tag{50}$$

Of course, there is no clear connection between the basis states $J_{\pi n}$ (or $J_{\nu n}$) occurring in IBA and PSM. However, for the limited purpose of examining the angular-momentum structure of the yrast band of ^{238}U, we will assume these basis states to be the same in the two models. With this assumption, the overlap term on the right-hand side is unity, and the overlap values given by Eq. (50) are 0.868, 0.865, 0.867, and 0.844, respectively, for the states with $J_n=0$, 2, 4, and 6.

The statistical significance of these overlaps can be estimated by calculating the probability $P(N:\rho)$ of obtaining an overlap equal to or greater than ρ between a given state (with N components) and another arbitrary state (with the same number of components). This probability is

$$P(N:\rho)\approx \sqrt{\frac{N}{2\pi}}\int_\rho^1 e^{-(1/2)Nx^2}dx. \tag{51}$$

Derivation of Eq. (51) is discussed in Ref. [11].

The number N_{J_n} of components $|[J_{\pi n}\times J_{\nu n}]J_n\rangle$ in $|\text{IBA:}J_n\rangle$ are $N_0=4$, $N_2=10$, $N_4=14$, and $N_6=16$. Between $|\text{IBA:}J_n\rangle$ and an arbitrary state $|J_n\rangle'$, the probabilities of obtaining overlap values greater than the given values are 1.9×10^{-2}, 2.3×10^{-3}, 5.8×10^{-4}, and 3.4×10^{-4}, respectively, for the $J_n=0$, 2, 4, and 6 states. In view of these small probabilities, the overlaps obtained between the IBA-2 and PSM states imply that the π-ν angular-momentum distributions in the n sector of the configuration space are similar in the two models. If the state $|\text{PSM:}J_n\rangle$ is truncated to contain the same number of components of the type $|[J_{\pi n}\times J_{\nu n}]J_n\rangle$ as are contained in $|\text{IBA:}J_n\rangle$ and the resulting state is normalized, the overlaps between $|\text{PSM:}J_n\rangle$ and $|\text{IBA:}J_n\rangle$ increase to 0.913, 0.913, 0.912, and 0.911, respectively, for the $J_n=0$, 2, 4, and 6 states with the probabilities of random occurrences decreasing to 1.1×10^{-2}, 1.2×10^{-3}, 2.3×10^{-4}, and 1.0×10^{-4}, respectively.

3. Distribution of yrast angular momentum over the n and a sectors

The total intrinsic state $\mathcal{F}$(IBA[30,0]) can be factored into n and a parts $\mathcal{F}^n$(IBA)[18,0]) and $\mathcal{F}^a$(IBA)[12,0]). Analogous to Eq. (47c), these states can be expanded as

$$\mathcal{F}^n(\text{IBA}[18,0]) = \sum_{J'_n} V^n_{J'_n}|J'_n\rangle, \tag{52a}$$

$$\mathcal{F}^a(\text{IBA}[12,0]) = \sum_{J'_a} V^a_{J'_a}|J'_a\rangle, \tag{52b}$$

$$\mathcal{F}(\text{IBA}[30,0]) = \sum_{J'} V_{J'}|J'\rangle. \tag{52c}$$

The yrast states $|J\rangle$ projected from $\mathcal{F}$(IBA[30,0]) are written as

$$|J\rangle = \sum_{J'_n,J'_a} A(\text{IBA:}J;J'_n,J'_a)|[J'_n\times J'_a]J\rangle, \tag{53}$$

where

$$P_3(\text{IBA:}J;J_n,J_a) \equiv |A(\text{IBA:}J;J_n,J_a)|^2 = \frac{|V^n_{J_n}V^a_{J_a}(J_nJ_a00J0)|^2}{|V_J|^2} \tag{54}$$

is the probability that $|J\rangle$ contains J_n and J_a. These probabilities are plotted in Figs. 7(a)–7(d) for the four lowest yrast states. The total J is spread out over a number of components $|[J_n\times J_a]J\rangle$(cf. Fig. 6 for PSM). The summed contributions $P_2(\text{IBA}J;J_a)$ are again similar, as shown in Fig. 5(b).

The probability that the total J of an yrast state arises entirely from bosons in the n states is given by

$$P_3(\text{IBA:}J;J_n=J,J_a=0) = \frac{|V^n_{J_n=J}V^a_{J_a=0}|^2}{|V_J|^2}. \tag{55}$$

These probabilities are plotted as a function of J in Fig. 8(a) by a dashed line. The full line in this figure shows the probabilities that, in addition to $J_a=0$, the angular momenta of π bosons and ν bosons in a states are individually coupled to zero [cf. Eq. (32)]. The latter probabilities never exceed $\sim$6%, whereas they are assumed to be 100% in PSM and FDSM. Thus, while the structures of IBA-2 states are similar to that of the PSM (see Sec. IV B 2 above) and the FDSM (see Sec. IV C below) over the n sector of configuration space, they are significantly different over the a sector.

C. Fermion dynamic symmetry model (FDSM)

In this model, the quadrupole collective states arise from (S_π,D_π) and (S_ν,D_ν) pairs in n states coupled to angular momenta 0 and 2. The number of protons and neutrons in the

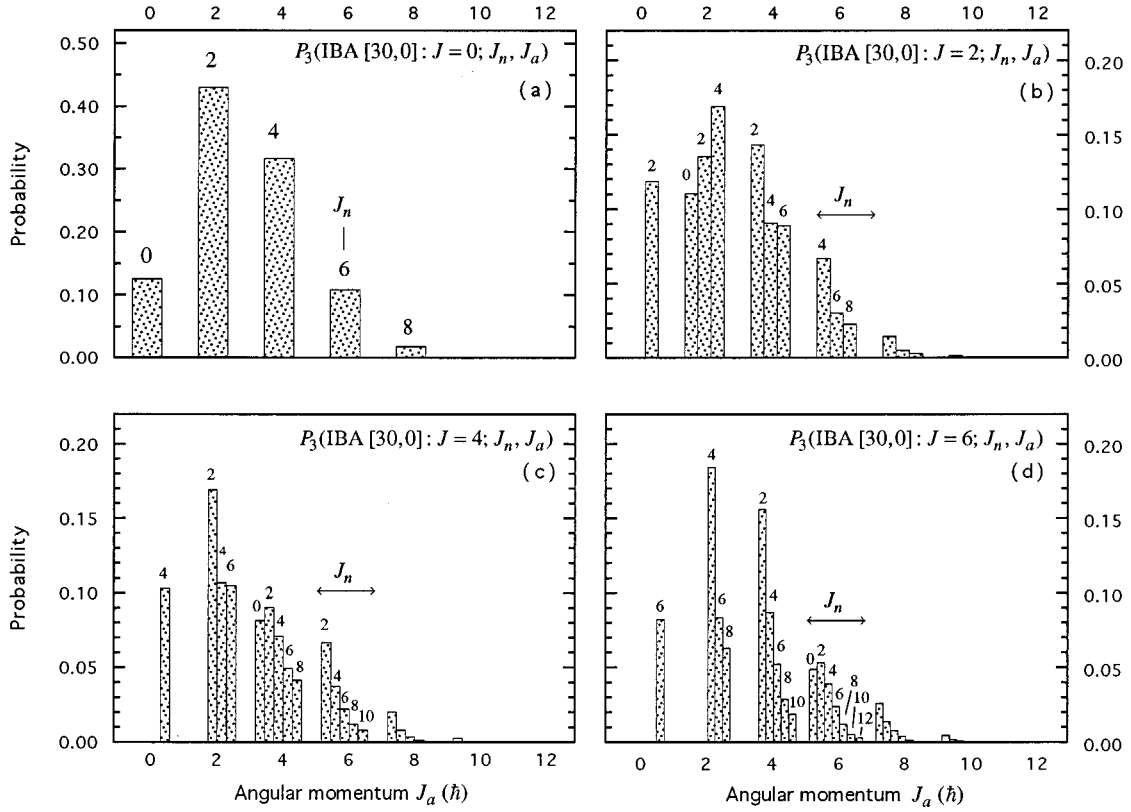

FIG. 7. P_3 distribution that the state $|J\rangle$ in ^{238}U contains the state $|[J_n \times J_a]J\rangle$ according to IBA.

n states are 6 and 12, respectively—the same as in the PSM. The pair degeneracies Ω_n, defined by $\Omega_n = \frac{1}{2}\Sigma_{j_n}(2j_n+1)$, are $\Omega_{\pi n}=15$ and $\Omega_{\nu n}=21$. According to FDSM, the SU_3 rep for the yrast band is given by $[\lambda=2N_n,0]$ if $N_n \leq \Omega_n/3$, where N_n is the number of pairs of n nucleons. For ^{238}U, the FDSM reps are $n\pi[6,0]$ and $n\nu[12,0]$; the total rep is therefore $n[18,0]$. These reps are the same as those of n bosons in IBA. In IBA, however, the total yrast band to which both n and a bosons contribute extends up to $J_{\max}=36$, whereas in the FDSM the collective part of the yrast band extends only up to the $J_{\max}=(J_n)_{\max}=18$ state. Yrast states with $J>18$ arise in FDSM as a result of contributions from degrees of freedom regarded as noncollective.

In the FDSM, the only collective mode of a protons and a neutrons is the mode of remaining in the state of seniority zero. The effective interactions can always be chosen to make this mode sufficiently stable under the influence of even the maximum quadrupole collectivity of n nucleons. Apart from mathematical simplicity, there are physical reasons for making this assumption; it helps, for instance, to extend the range of deformed nuclei for which axially symmetric reps can occur in FDSM.

D. Projected single-shell asymptotic Nilsson model (projected SSANM)

The basic assumption of this model is that the yrast states are well described by the band of states of definite J projected from the asymptotic Nilsson intrinsic state within a major shell. We list the maximum values of angular momenta of protons and neutrons in the n and a sectors of this intrinsic state. The distributions of angular momenta in these sectors are then calculated. We bring out in some detail the SU_3-like behavior of the a nucleons. Finally, we illustrate the collective distribution of the total J of an yrast state over both J_n and J_a states.

1. The asymptotic Nilsson intrinsic state

The deformed sp Nilsson states $\phi_k^\alpha(\beta)$ are eigenstates of the Nilsson Hamiltonian

$$h(\beta)=h_0-\beta\,\hbar\omega_0 r^2 Y_0^2, \tag{56}$$

where β is the deformation parameter, $\hbar\omega_0=41A^{-1/3}$ MeV, and r^2 is in units of the harmonic oscillator length parameter α^2. The spherical Hamiltonian h_0 has the eigenstates ψ_k^j with sp energies ϵ_j. For each value of β, the Nilsson eigenstate $\phi_k^\alpha(\beta)$ can be obtained by diagonalizing $h(\beta)$ with the spherical states ψ_k^j (within a single major shell) as basis states. The resulting eigenstates $\phi_k^\alpha(\beta)$ can be expanded, as in Eq. (1), in terms of ψ_k^j. When h_0 is specified by the empirically determined sp energies ϵ_j, the coefficients $c_{j,k}^\alpha(\beta)$ of the expansion change rapidly with β for small β. As β is increased, these coefficients approach asymptotically the values obtained by taking the sp energies ϵ_j to be degenerate. For sufficiently large deformations (say, $\beta>0.15$), the energy eigenvalues $\epsilon_k^\alpha(\beta)$ of the single-shell Nilsson states vary linearly with β. The states ϕ_k^α, obtained by diagonalizing $h(\beta)$ with the sp energies taken to be degenerate, are defined to be asymptotically deformed sp states. These states are also eigenstates of $r^2Y_0^2$ and can be

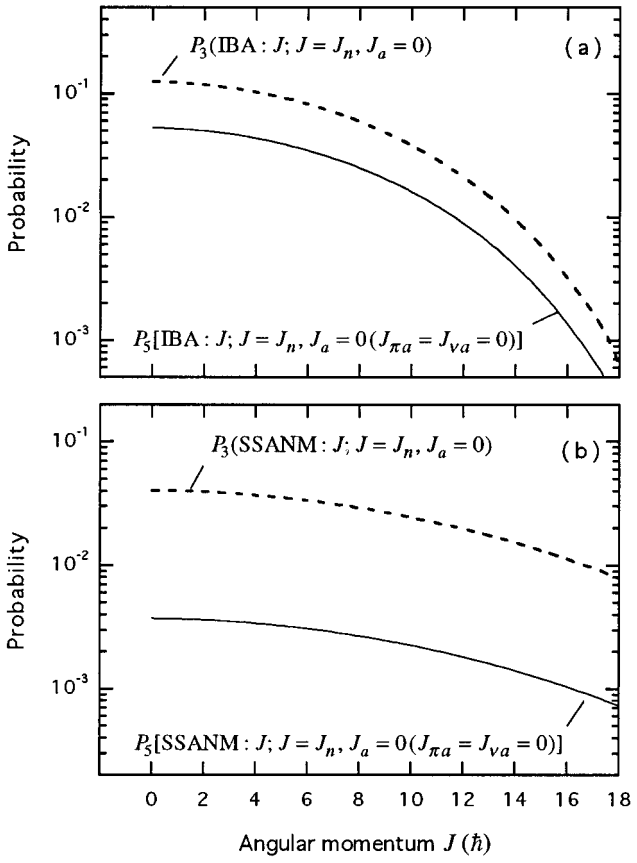

FIG. 8. Dashed curve shows the P_3 distribution if the state $|J\rangle$ in ^{238}U arises entirely from (a) bosons in the n states of IBA and (b) nucleons in the n states of SSANM. Solid curves show the probability distributions P_5 that result if $J_{\pi a}=0$ and $J_{\nu a}=0$ in addition to $J_a=0$.

labeled by the eigenvalues $q_k^\alpha=\langle\phi_k^\alpha|r^2Y_0^2|\phi_k^\alpha\rangle$ of the quadrupole moment. The state with a larger value of q_k^α has a lower energy eigenvalue ϵ_k^α.

In Tables I, II, and III, we list the expansion coefficients $c_{j,k}^\alpha$ for all asymptotically deformed states ϕ_k^α in the 50–82, 82–126, and 126–184 shells, respectively. The states are listed in order of decreasing values of q_k^α. In evaluating q_k^α, harmonic-oscillator wave functions were used for the radial part of ψ_k^j. Only those coefficients for positive values of k are listed; those for negative values of k are given by Eq. (2). In addition, $q_k^\alpha=q_{-k}^\alpha$. Some details concerning the calculation of q_k^α are given in the Appendix.

The SSANM is based on the ansatz ''a nucleus is as deformed as it can be in a *single* major shell.'' This ansatz is supported by our previous demonstration [20] that $B(E2;0_1^+\rightarrow 2_1^+)$ values for even-even nuclei calculated using the asymptotically deformed Nilsson intrinsic state are in good agreement with measured values. In view of this agreement, we expect the states of definite J projected from this intrinsic state to provide a good description of the yrast band.

The intrinsic Nilsson state of ^{238}U is obtained by placing sequentially the 10 valence protons and 20 valence neutrons in the eigenstates ϕ_k^α with the largest available eigenvalues q_k^α consistent with the Pauli principle. Accordingly, protons occupy (see Table II) six n states with $k_n=\pm\frac{1}{2}^-$, $\pm\frac{1}{2}^-$, and $\pm\frac{3}{2}^-$ and four a states with $k_a=\pm\frac{1}{2}^+$ and $\pm\frac{3}{2}^+$. The 20 valence neutrons are similarly placed (see Table III) in 12 n states with $k_n=\pm\frac{1}{2}^+$, $\pm\frac{1}{2}^+$, $\pm\frac{3}{2}^+$, $\pm\frac{3}{2}^+$, $\pm\frac{1}{2}^+$, and $\pm\frac{5}{2}^+$ and in 8 a states with $k_a=\pm\frac{1}{2}^-$, $\pm\frac{3}{2}^-$, $\pm\frac{5}{2}^-$, and $\pm\frac{7}{2}^-$.

TABLE I. Quadrupole operator eigenvalues $\langle q_k\rangle$ and expansion coefficients $c_{j_k}^\alpha$ for the asymptotically deformed sp states in the 50–82 shell listed in the order of decreasing quadrupole moments. α enumerates eigenstates belonging to a given k. Only values for positive k are given. For negative k, the symmetry relation $c_{j_{-k}}=(-)^{j-k}c_{j_k}$ applies. PSM values are for the $[\tilde{\lambda},0]=[3,0]$ representation. For abnormal-parity states, the $\langle q_k\rangle$ SSANM moments are in brackets. There are no corresponding PSM moments. $\alpha=1$ label is implicit for all abnormal-parity states.

α	k	$\langle q_k\rangle$ PSM	$\langle q_k\rangle$ SSANM	$c^\alpha_{(7/2)k}$	$c^\alpha_{(5/2)k}$	$c^\alpha_{(3/2)k}$	$c^\alpha_{(1/2)k}$	$c^1_{(11/2)k}$
1	$\frac{1}{2}$	6	7.379	-0.417	-0.483	0.600	0.483	
2	$\frac{1}{2}$	3	3.849	0.646	-0.609	-0.313	0.337	
1	$\frac{3}{2}$	3	3.520	0.737	0.495	-0.46		
	$\frac{1}{2}$		(3.182)					1
	$\frac{3}{2}$		(2.636)					1
	$\frac{5}{2}$		(1.545)					1
2	$\frac{3}{2}$	0	0.238	-0.586	0.807	-0.071		
	$\frac{7}{2}$		(-0.091)					1
3	$\frac{1}{2}$	0	-0.165	0.593	0.485	0.579	0.278	
1	$\frac{5}{2}$	0	-0.192	0.948	0.318			
	$\frac{9}{2}$		(-2.273)					1
2	$\frac{5}{2}$	-3	-3.475	-0.318	0.948			
3	$\frac{3}{2}$	-3	-3.758	0.336	0.332	0.885		
1	$\frac{7}{2}$	-3	-3.667	1				
4	$\frac{1}{2}$	-3	-3.730	-0.239	0.400	-0.455	0.759	
	$\frac{11}{2}$		(-5)					1

Once the number of nucleons in the n states is determined on the basis of increasing energy values from the Nilsson diagram (at the physical deformation of the nucleus), the PSM and FDSM assign to these nucleons the most deformed SU_3 rep available. In our SSANM approach, we construct the most deformed Nilsson intrinsic state of all nucleons first and then determine the number of nucleons in n and a states based on decreasing q_k^α values. The two procedures generally give the same occupancy numbers.

The effect of pairing is neglected in the SSANM (just as it is in the PSM and FDSM for nucleons in the n states) by arguing that it is reasonable, as a first approximation, to ignore pairing for nucleons in a well-deformed mean field. This is particularly true for models in which the moment of inertia of the rotational band can be varied independently of deformation as it can be in the PSM and FDSM.

2. Angular momentum content of the intrinsic state

The intrinsic states of protons and neutrons in ^{238}U can be regarded as superpositions of states with definite angular mo-

TABLE II. Quadrupole operator matrix elements $\langle q_k \rangle$ and expansion coefficients $c^{\alpha}_{j_k}$ for the asymptotically deformed sp states in the 82–126 shell. PSM values are for the $[\tilde{\lambda},0]=[4,0]$ representation. Also see caption for Table I.

α	k	$\langle q_k \rangle$ PSM	$\langle q_k \rangle$ SSANM	$c^{\alpha}_{(9/2)k}$	$c^{\alpha}_{(7/2)k}$	$c^{\alpha}_{(5/2)k}$	$c^{\alpha}_{(3/2)k}$	$c^{\alpha}_{(1/2)k}$	$c^{1}_{(13/2)k}$
1	$\frac{1}{2}$	8	9.596	-0.290	-0.407	0.518	0.543	-0.433	
2	$\frac{1}{2}$	5	6.173	0.539	-0.516	-0.498	0.435	0.076	
1	$\frac{3}{2}$	5	5.898	-0.558	-0.504	0.571	0.331		
	$\frac{1}{2}$		(3.692)						1
	$\frac{3}{2}$		(3.231)						1
2	$\frac{3}{2}$	2	2.703	-0.623	0.667	0.187	-0.343		
	$\frac{5}{2}$		(2.308)						1
3	$\frac{1}{2}$	2	2.243	0.647	0.496	0.196	0.105	-0.534	
1	$\frac{5}{2}$	2	2.184	0.812	0.433	-0.393			
	$\frac{7}{2}$		(0.923)						1
2	$\frac{5}{2}$	-1	-0.896	-0.504	0.858	-0.096			
	$\frac{9}{2}$		(-0.923)						1
4	$\frac{1}{2}$	-1	-1.340	-0.420	0.497	-0.519	0.539	-0.131	
1	$\frac{7}{2}$	-1	-1.358	0.965	0.261				
3	$\frac{3}{2}$	-1	-1.434	0.523	0.386	0.730	0.210		
	$\frac{11}{2}$		(-3.231)						1
2	$\frac{7}{2}$	-4	-4.551	-0.261	0.965				
1	$\frac{9}{2}$	-4	-4.727	1					
4	$\frac{3}{2}$	-4	-4.803	-0.163	0.372	-0.326	0.854		
3	$\frac{5}{2}$	-4	-4.834	0.296	0.276	0.915			
5	$\frac{1}{2}$	-4	-4.854	0.175	0.273	0.420	0.463	0.710	
	$\frac{13}{2}$		(-6)						1

menta J_π and J_ν. The minimum value of J_π or J_ν is zero. The maximum value of J_π is equal to the maximum possible value M_π of the projection of total angular momentum along the space-fixed z axis. The maximum M_π value is obtained by assigning protons to the spherical states ψ^j_m with the largest available value of m consistent with the Pauli principle. For the n protons in the 82–126 shell, the largest m value ($m=\frac{9}{2}$) belongs to the $h_{9/2}$ state with the largest j value. The value $m=\frac{7}{2}$ is contributed by the $h_{9/2}$ and $g_{7/2}$ states. The next smaller value $m=\frac{5}{2}$ is contributed by the $h_{9/2}$, $g_{7/2}$, and $d_{5/2}$ states. Hence, the maximum possible $M_{\pi n}$ value for six n protons is $(M_{\pi n})_{\max}=\frac{9}{2}+\frac{7}{2}+\frac{7}{2}+\frac{5}{2}+\frac{5}{2}+\frac{5}{2}=19$, and hence $(J_{\pi n})_{\max}=19$. Reflection symmetry imposed on the intrinsic state allows it to contain only even angular momenta. Therefore, the intrinsic state of six n-protons will contain states with $J_\pi=0,2,\ldots$ up to $J_\pi=18$.

Although states like $h_{9/2,m=9/2}$, $h_{9/2,m=7/2},\ldots$ are not explicitly present in the intrinsic state listed in Sec. IV D 1, they are generated from the intrinsic state by the projection procedure described in Sec. II B.

Similarly, the maximum value of the angular momentum of four protons in the $i_{13/2}$ state is $(J_{\pi a})_{\max}=\frac{13}{2}+\frac{11}{2}+\frac{9}{2}+\frac{7}{2}=20$, and the intrinsic state will contain states with $J_{\pi a}=0,2,\ldots,20$. Corresponding values for the neutrons are $(J_{\nu n})_{\max}=36$ for 12 n neutrons and $(J_{\nu a})_{\max}=32$ for 8 a neutrons. The yrast band projected from the Nilsson intrinsic state extends up to $J_{\max}=106$ composed of $(J_n)_{\max}=54$ and $(J_a)_{\max}=52$.

3. Distribution of angular momenta in different sectors of the intrinsic state

The intrinsic state can be factored into four parts $\mathcal{F}^{\pi n}_{K_{\pi n}}$, $\mathcal{F}^{\pi a}_{K_{\pi a}}$, $\mathcal{F}^{\nu n}_{K_{\nu n}}$, and $\mathcal{F}^{\nu a}_{K_{\nu a}}$ consisting of (6×6), (4×4), (12×12), and (8×8) Slater determinants, respectively. These parts, in turn, can be expanded as

$$\mathcal{F}^{\pi n}_{K_{\pi n}}=\sum_{J'_{\pi n}} W^{\pi n}_{J'_{\pi n},K_{\pi n}}|J'_{\pi n}\rangle, \quad J'_{\pi n}=0,2,\ldots,18, \tag{57a}$$

$$\mathcal{F}^{\pi a}_{K_{\pi a}}=\sum_{J'_{\pi a}} W^{\pi a}_{J'_{\pi a},K_{\pi a}}|J'_{\pi a}\rangle, \quad J'_{\pi a}=0,2,\ldots,20, \tag{57b}$$

$$\mathcal{F}^{\nu n}_{K_{\nu n}}=\sum_{J'_{\nu n}} W^{\nu n}_{J'_{\nu n},K_{\nu n}}|J'_{\nu n}\rangle, \quad J'_{\nu n}=0,2,\ldots,36, \tag{57c}$$

TABLE III. Quadrupole operator matrix elements $\langle q_k \rangle$ and expansion coefficients $c^{\alpha}_{j_k}$ for the asymptotically deformed sp states in the 126–184 shell. PSM values are for the $[\tilde{\lambda},0]=[5,0]$ representation. Also see caption for Table I.

α	k	$\langle q_k \rangle$ PSM	$\langle q_k \rangle$ SSANM	$c^{\alpha}_{(11/2)k}$	$c^{\alpha}_{(9/2)k}$	$c^{\alpha}_{(7/2)k}$	$c^{\alpha}_{(5/2)k}$	$c^{\alpha}_{(3/2)k}$	$c^{\alpha}_{(1/2)k}$	$c^{1}_{(15/2)k}$
1	$\frac{1}{2}$	10	11.742	-0.202	-0.335	0.420	0.525	-0.485	-0.399	
2	$\frac{1}{2}$	7	8.409	-0.425	0.440	0.548	-0.473	-0.285	0.146	
1	$\frac{3}{2}$	7	8.207	-0.411	-0.471	0.560	0.463	-0.286		
2	$\frac{3}{2}$	4	5.042	0.577	-0.565	-0.394	0.437	0.037		
3	$\frac{1}{2}$	4	4.602	0.612	0.485	-0.134	-0.071	-0.487	-0.361	
1	$\frac{5}{2}$	4	4.549	0.648	0.482	-0.534	-0.251			
	$\frac{1}{2}$		(4.200)							1
	$\frac{3}{2}$		(3.800)							1
	$\frac{5}{2}$		(3.000)							1
	$\frac{7}{2}$		(1.800)							1
2	$\frac{5}{2}$	1	1.580	-0.584	0.732	0.109	-0.333			
4	$\frac{1}{2}$	1	1.055	0.533	-0.516	0.350	-0.279	-0.229	0.444	
1	$\frac{7}{2}$	1	0.961	0.857	0.379	-0.348				
3	$\frac{3}{2}$	1	0.901	0.616	0.418	0.426	0.152	-0.492		
	$\frac{9}{2}$		(0.2)							1
	$\frac{11}{2}$		(-1.800)							1
2	$\frac{7}{2}$	-2	-2.006	-0.439	0.892	-0.111				
1	$\frac{9}{2}$	-2	-2.469	0.975	0.221					
4	$\frac{3}{2}$	-2	-2.469	-0.315	0.489	-0.447	0.659	-0.162		
3	$\frac{5}{2}$	-2	-2.586	0.474	0.333	0.799	0.161			
5	$\frac{1}{2}$	-2	-2.594	0.329	0.372	0.558	0.450	0.473	0.125	
	$\frac{13}{2}$		(-4.200)							1
2	$\frac{9}{2}$	-5	-5.608	-0.221	0.975					
1	$\frac{11}{2}$	-5	-5.769	1						
4	$\frac{5}{2}$	-5	-5.851	-0.121	0.348	-0.254	0.894			
3	$\frac{7}{2}$	-5	-5.878	0.269	0.248	0.931				
6	$\frac{1}{2}$	-5	-5.906	-0.109	0.231	-0.268	0.464	-0.413	0.691	
5	$\frac{3}{2}$	-5	-5.911	0.141	0.213	0.387	0.370	0.805		
	$\frac{15}{2}$		(-7)							1

$$\mathcal{F}^{\nu a}_{K_{\nu a}} = \sum_{J'_{\nu a}} W^{\nu a}_{J'_{\nu a},K_{\nu a}} |J'_{\nu a}\rangle, \quad J'_{\nu a}=0,2,\ldots,32. \quad (57d)$$

The distributions $P_1(\text{SSANM}:J_{\pi n})$, $P_1(\text{SSANM}:J_{\pi a})$, $P_1(\text{SSANM}:J_{\nu n})$, and $P_1(\text{SSANM}:J_{\nu a})$ in the corresponding intrinsic states are given by the squares $|W^{\pi n}_{J_{\pi n},K_{\pi n}}|^2$, $|W^{\pi a}_{J_{\pi a},K_{\pi a}}|^2$, $|W^{\nu n}_{J_{\nu n},K_{\nu n}}|^2$, and $|W^{\nu a}_{J_{\nu a},K_{\nu a}}|^2$, respectively. To determine these expansion coefficients, we first use the deformed sp states listed in Tables II and III to calculate the functions $\langle \mathcal{F}_K | e^{-i\beta J_y} | \mathcal{F}_K \rangle$ [see Eq. (10)]. For each of these functions, the integral in Eq. (14) is carried out to calculate the corresponding $|W|^2$ value.

4. Normal-parity sector

The distributions $P_1(\text{SSANM}:J_{\pi n})$, $P_1(\text{SSANM}:J_{\nu n})$, and $P_1(\text{SSANM}:J_n)$ in the n states $\mathcal{F}^{\pi n}$, $\mathcal{F}^{\nu n}$, and $\mathcal{F}^{n}$ are shown in Figs. 9(a)–9(c). Also shown there are the corresponding P_1 distributions from PSM. These comparisons show that the PSM intrinsic state is an excellent approximation to the SSANM intrinsic state in the n sector.

5. SU_3-like behavior of the abnormal-parity sector

The distributions of angular momenta in the a states $\mathcal{F}^{\pi a}_{K_{\pi a}}$, $\mathcal{F}^{\nu a}_{K_{\nu a}}$, and $\mathcal{F}^{a}_{K_a}$ are shown in Figs. 10(a)–10(c). In this case there is no underlying SU_3 symmetry. However, in the same figures, we compare these distributions with those corresponding to the SU_3 reps $\pi a[20,0]$, $\nu a[32,0]$, and $a[52,0]$ which contain the same angular momenta as the Nilsson states. The distributions are similar.

The overlaps between (i) $\mathcal{F}^{\pi a}_{K_{\pi a}}(\text{SSANM})$ and $\mathcal{F}^{\pi a}_{K_{\pi a}}[20,0]$, (ii) $\mathcal{F}^{\nu a}_{K_{\nu a}}(\text{SSANM})$ and $\mathcal{F}^{\nu a}_{K_{\nu a}}[32,0]$, and (iii)

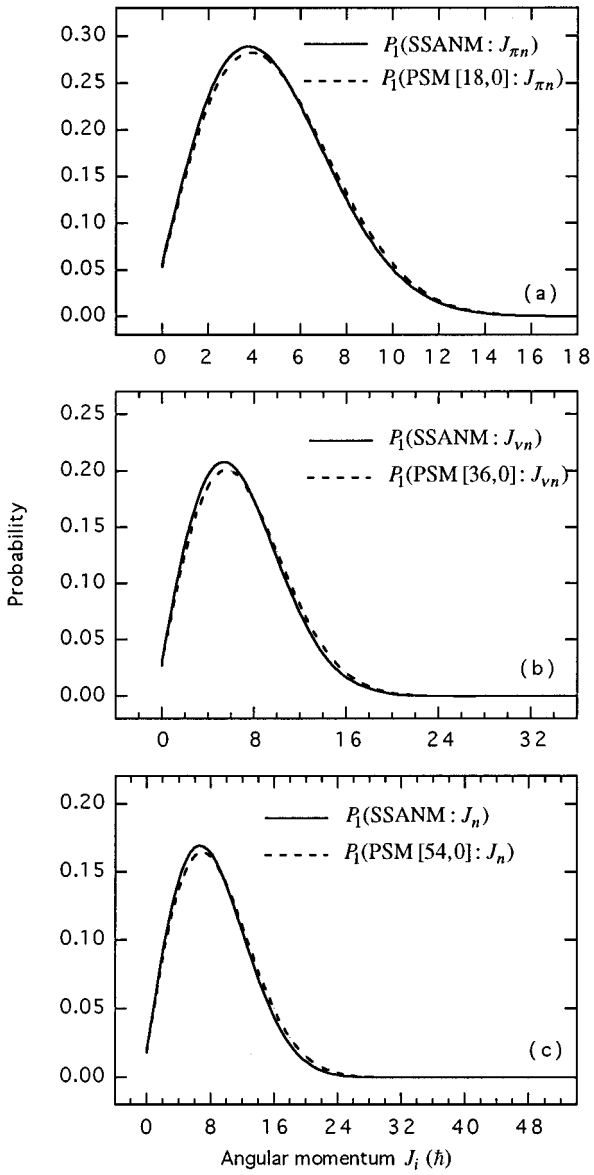

FIG. 9. P_1 distributions of nucleons in the n states compared for SSANM and PSM. The abscissa is $J_{\pi n}$ in (a), $J_{\nu n}$ in (b), and J_n in (c). These results are for ^{238}U.

$\mathcal{F}^a_{K_a}$(SSANM) and $\mathcal{F}^a_{K_a}[52,0]$ are found to be 0.990, 0.987, and 0.999, respectively. The state $\mathcal{F}^{\pi a}_{K_{\pi a}}$ has 11 components $|J_{\pi a}\rangle$ with $J_{\pi a}=0,2,4,\ldots,20$. Similarly, the states $\mathcal{F}^{\nu a}_{K_{\nu a}}$ and $\mathcal{F}^a_{K_a}$ have 17 and 27 components, respectively. The probabilities $P(N:\rho)$ of randomly obtaining these overlap values are $P(11:0.990)=2.1\times10^{-3}$, $P(17:0.987)=8.9\times10^{-5}$, and $P(27:0.999)=5.4\times10^{-7}$.

Although the *distributions* of $J_{\pi a}$ and $J_{\nu a}$ in the Nilsson intrinsic state are SU_3-like, the quadrupole moments of the a nucleons in this intrinsic state are much smaller than expected on the basis of this similarity. From the effective values $\lambda_{\pi a}=20$ and $\lambda_{\nu a}=32$, the expected moments are $Q_{\pi a}[20,0]=40$ and $Q_{\nu a}[32,0]=64$ in units of α^2. The values obtained using the q_k values from Tables II and III are $Q_{\pi a}(\text{SSANM})=13.8$ and $Q_{\nu a}(\text{SSANM})=25.6$ in the same units. Thus, the quadrupole collectivity of the a nucleons is only $\sim$40% of the value expected on the basis of SU_3 symmetry.

Instead of using the highest J contained in the Nilsson state of a nucleons to determine the value of λ for the effective SU_3 rep $[\lambda,0]$, we may choose λ such that the average value $\overline{J}(\lambda)$ is closest to the value of $\overline{J}$(SSANM) for the Nilsson intrinsic state. For ^{238}U, such SU_3 reps are found to be $\pi[22,0]$ and $\nu[24,0]$. As shown in Figs. 10(d) and 10(e), the $P_1(SU_3)$ distributions for these reps are indeed close to the corresponding SSANM ones. The new value of $\lambda_\pi=22$ is close to the value 20 deduced from $(J_\pi)_{\max}$, but $\lambda_\nu=24$ is significantly smaller than $(J_\nu)_{\max}=36$.

As shown in Fig. 10(f), the P_1(SSANM) distribution of J_a in the combined intrinsic state of the 12 nucleons in the a sector is so well reproduced by the distribution of the effective SU_3 rep $a[46,0]$ that the two curves in Fig. 10(f) are hardly distinguishable. It is not *a priori* obvious why the $P_1(SU_3)$ distributions of J in an SU_3 rep $[\lambda,0]$ for which the $\overline{J}(\lambda)$ value is closest to the $\overline{J}$(SSANM) value should agree as well with the P_1(SSANM) distributions as they do [see Figs. 10(d)–10(f)].

6. Collective distribution of the total angular momentum over the n and a sectors

The intrinsic states $\mathcal{F}^n_{K_n}$, $\mathcal{F}^a_{K_a}$, and $\mathcal{F}_K$ can be written as

$$\mathcal{F}^n_{K_n}=\sum_{J'_n} W^n_{J'_n}|J'_n\rangle, \quad J'_n=0,2,\ldots,54, \tag{58a}$$

$$\mathcal{F}^a_{K_a}=\sum_{J'_a} W^a_{J'_a}|J'_a\rangle, \quad J'_a=0,2,\ldots,52, \tag{58b}$$

$$\mathcal{F}_K=\sum_{J'} W_{J'}|J'\rangle, \quad J'=0,2,\ldots,106. \tag{58c}$$

We show in Fig. 11 the distribution $|W_J|^2$ of the total J in the Nilsson intrinsic state. If this distribution is compared, as in Fig. 11, with the corresponding one obtained for the SU_3 [106,0] rep, the two distributions are remarkably close over 27 orders of magnitude. This similarity is surprising because unlike the n nucleons the a nucleons—which contribute about half of the total angular momentum—do not have SU_3 symmetry. The overlap $\langle\mathcal{F}(SU_3[106,0]|\mathcal{F}(\text{SSANM})\rangle$ is 0.9998. With $N=54$ components, the probability of random occurrence is 1.1×10^{-15}.

The state $|J\rangle$ projected from the Nilsson intrinsic state, factored into n and a parts, can be written as

$$|J\rangle=\sum_{J'_n,J'_a} A(\text{SSANM}:J;J'_n,J'_a)|[J'_n\times J'_a]J\rangle, \tag{59}$$

where

$$P_3(\text{SSANM}:J;J_n,J_a)\equiv|A(\text{SSANM}:J;J_n,J_a)|^2 = \frac{|W^n_{J_n}W^a_{J_a}(J_nJ_a00J0)|^2}{|W_J|^2}. \tag{60}$$

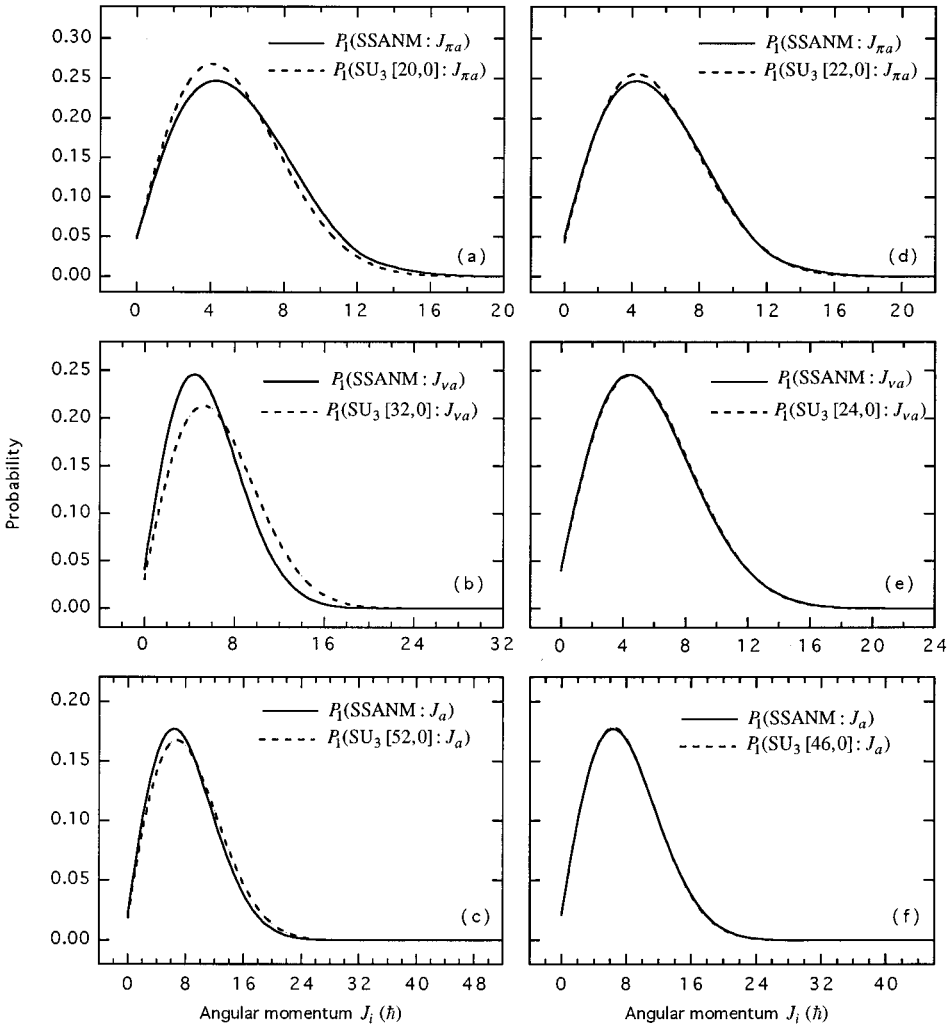

FIG. 10. P_1 distributions of nucleons in the a states of SSANM showing their SU_3-like behavior. The abscissa is $J_{\pi a}$ in (a) and (d), J_{va} in (b) and (e), and J_a in (c) and (f). These results are for ^{238}U.

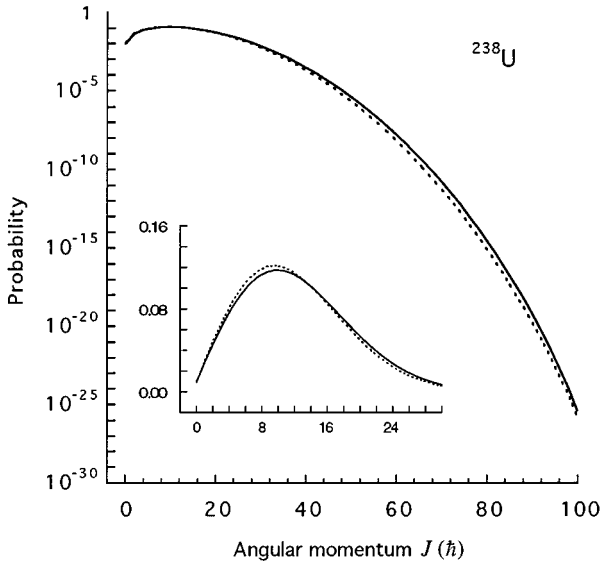

FIG. 11. P_1 distribution for the total SSANM intrinsic state (dashed curve) compared with that for an SU_3 representation [106,0] (full curve) for ^{238}U. The inset shows the early portion of the figure on a linear vertical scale.

These probability distributions are shown in Figs. 12(a)–12(d) and P_2(SSANM:$J;J_a$) distributions in Fig. 5(c). A decomposition of J into either J_π and J_ν or J_n and J_a will *ipso facto* result in broad distributions (see, for example, Figs. 4, 7, and 12) provided that both sectors are allowed to share the same mean field. The consequence of not allowing the a nucleons to do so results in what is shown in Fig. 6 which is drastically different from the results shown in Figs. 4, 7, and 12.

The P_3 distributions such as those shown in Figs. 12(a)–12(d) become so complex for higher J values that a three-dimensional view is required to convey adequately the fragmentation of the total J into J_n and J_a. Figure 13 shows this fragmentation for the $J=10$ state in ^{238}U. In PSM, the probability bar corresponding to $J_n=10$, $J_a=0$, marked by an arrow, becomes unity, and all other probabilities are set to zero.

In Fig. 8(b) we present $P_3(J;J_n,J_a=0)$ and $P_5[J;J_n,J_a=0\,(J_{\pi a}=J_{\nu a}=0)]$ for SSANM. They show that if the Nilsson intrinsic state is a good description of the intrinsic state of ^{238}U, the probability that the a protons and a neutrons are individually coupled to angular momentum zero in a yrast state J is $<0.4\%$ and decreases with J. The states $|J_{\pi a}=0\rangle$ and $|J_{\nu a}=0\rangle$ projected from the Nilsson intrinsic state do not have definite seniority. Hence, the prob-

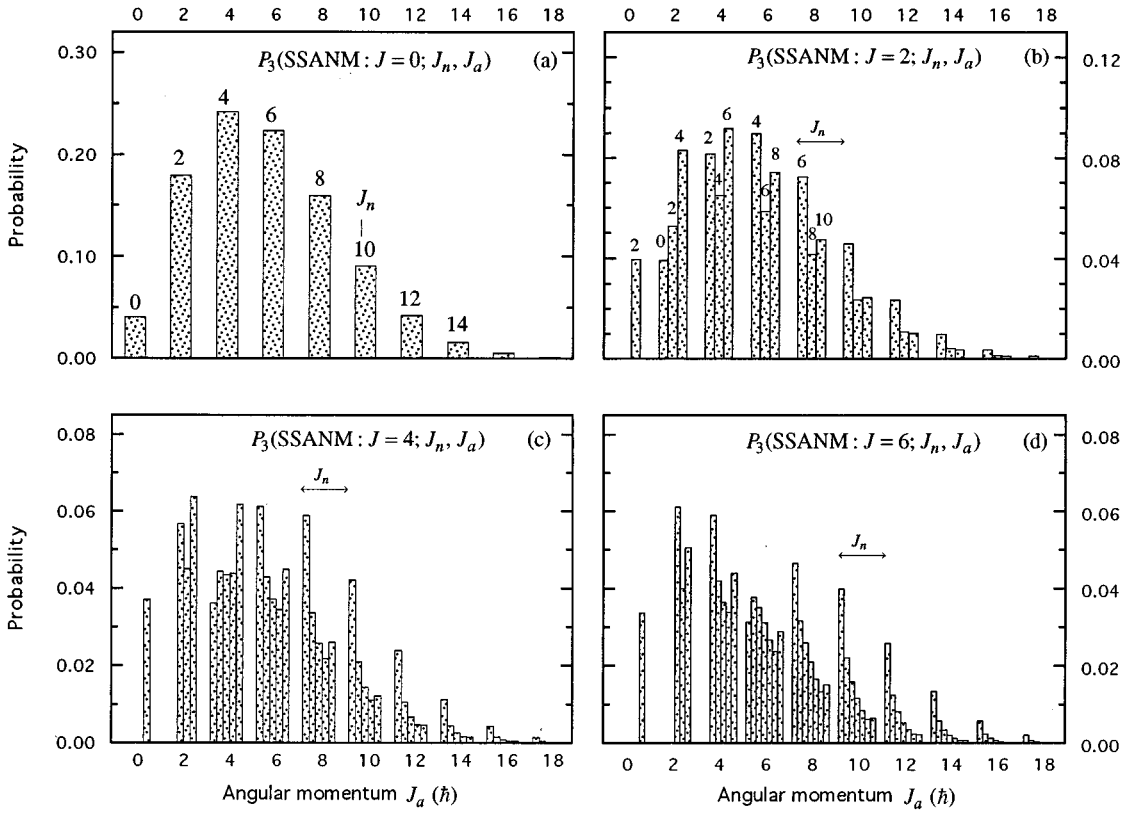

FIG. 12. P_3 distribution that a particular yrast state $|J\rangle$ in ^{238}U contains the state $|[J_n \times J_a]J\rangle$ according to SSANM.

ability that the a nucleons have seniority zero in the yrast band is even smaller.

In Sec. IV B 2, we calculated the overlaps between the states $|\text{IBA}{:}J_n\rangle$ and $|\text{PSM}{:}J_n\rangle$ in the n sector. We now do the same between the states $|\text{IBA}{:}J_a\rangle$ and $|\text{SSANM}{:}J_a\rangle$ in the a sector. The number N_{Ja} of components $|[J_{\pi a} \times J_{\nu a}]J_a\rangle$ in the IBA states are $N_0=3$, $N_2=7$, $N_4=9$, and $N_6=8$ for the $J_a=0$, 2, 4, and 6 states, respectively. The corresponding numbers of components in the states $|\text{SSANM}{:}J_a\rangle$ are $N_0=11$, $N_2=31$, $N_4=49$, and

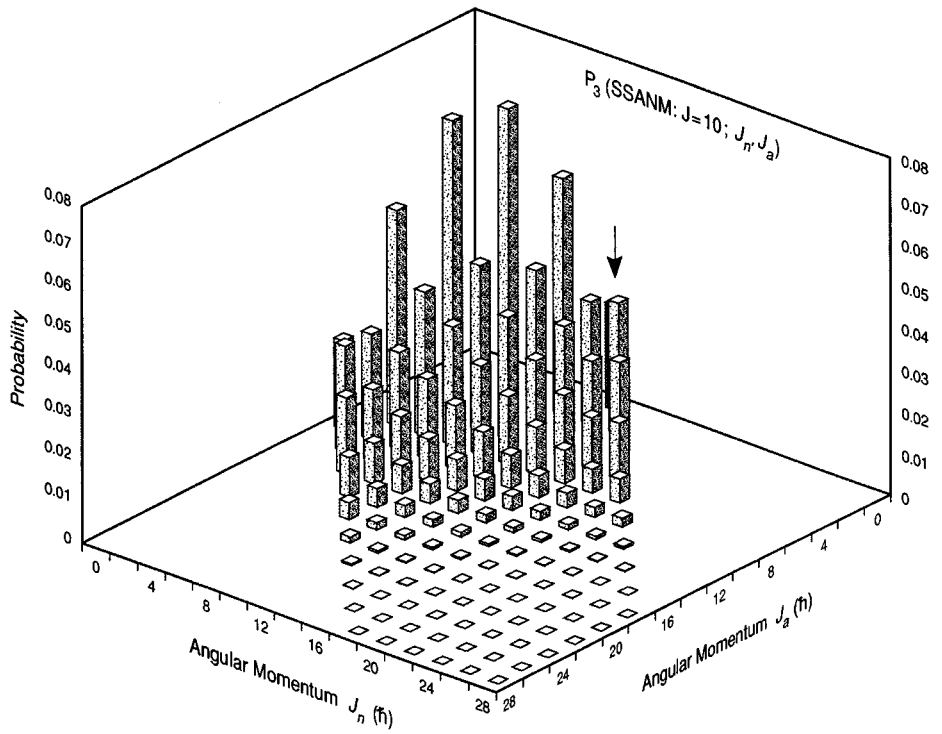

FIG. 13. A three-dimensional view of the P_3 distribution that the yrast state $|J\rangle$ with $J=10$ in ^{238}U contains the state $|[J_n \times J_a]J\rangle$ according to SSANM.

$N_6=65$. The overlaps $\langle \text{IBA}:J_a|\text{SSANM}:J_a\rangle$ are 0.66, 0.68, 0.70, and 0.72, respectively, for the $J_a=0, 2, 4,$ and 6 states. The probabilities of randomly getting these values are 0.09, 0.03, 0.02, and 0.02, respectively. These overlaps are relatively small because N(SSANM) is much larger than N(IBA). If the states $|\text{SSANM}:J_a\rangle$ are truncated to contain the same numbers of components $|[J_{\pi a}\times J_{\nu a}]J_a\rangle$ as occur in IBA and then normalized, the overlaps of these truncated and normalized SSANM states increase to 0.79, 0.82, 0.88, and 0.94 while the probabilities of random occurrences decrease to 0.05, 0.01, 0.003, and 0.002, respectively, for the $J_a=0, 2, 4,$ and 6 states.

V. STRUCTURE OF THE YRAST BAND OF $^{168}_{68}\text{Er}_{100}$

In PSM and FDSM, the structure of ^{168}Er is more complex than that of ^{238}U. In the PSM, the SU_3 reps of valence nucleons in ^{168}Er are triaxial ($\mu\neq 0$). In the FDSM, the complexity has two origins: (i) SU_3 symmetry is possible only for valence neutrons with the available rep being [18,0] and (ii) valence protons have SO(6) symmetry [6]. Because there is no single overall symmetry for both protons and neutrons, the structure of the yrast band has to be obtained by explicitly carrying out a diagonalization of the FDSM Hamiltonian. In the SSANM, we shall associate the yrast band of ^{168}Er with the states projected from the most deformed Nilsson intrinsic state, as was done for ^{238}U.

The highest angular momentum of the yrast band observed experimentally in ^{168}Er till now is $J_{\max}=18$ [23]. In shell models, this band results from the interaction between 18 valence protons and 18 valence neutrons. The former occupy the spherical sp states $(0g_{7/2}, 1d_{5/2})$, $(1d_{3/2}, 2s_{1/2})$ of n parity and $0h_{11/2}$ of a parity in the 50–82 shell. The latter occupy the states $(0h_{9/2}, 1f_{7/2})$, $(1f_{5/2}, 2p_{3/2})$, $2p_{3/2}$ of n parity and $0i_{13/2}$ of a parity in the 82–126 shell.

A. Pseudo-SU_3 model (PSM)

The Nilsson diagram (of the energies of deformed sp states) for ^{168}Er at $\beta\approx 0.25$ shows that 10 protons are in the n states and 8 in the $h_{11/2}$ state. Similarly, the number of neutrons in the n and a states are also 10 and 8, respectively. The pseudo-SU_3 reps for the n nucleons are $[\tilde{\lambda}_\pi,\tilde{\mu}_\pi]=[10,4]$ and $[\tilde{\lambda}_\nu,\tilde{\mu}_\nu]=[20,4]$. Both reps have triaxial intrinsic states containing bands with $K=0,2,$ and 4 in the Elliott classification (or $\kappa=0, 2,$ and 4 in the Vergados orthogonal classification). The $K_{\pi n}=0$ yrast band contains states with $J_{\pi n}=0,2,\ldots,14$ and the $K_{\nu n}=0$ band states with $J_{\nu n}=0,2,\ldots,24$. The total pseudo-SU_3 rep of ^{168}Er is [30,8] with the $K_n=0$ band containing states with $J_n=0,2\ldots,38$. The yrast band is generally associated with the $K=0$ band and we confine our discussion to the distribution of angular momenta only in this band. These distributions, normalized to unity, are shown in Figs. 14(a)–14(c) for the proton, neutron, and coupled reps. In the PSM, the 16 nucleons in the a states are assumed to contribute zero angular momentum; therefore, the total angular momentum is generated only by the n nucleons (that is, $J=J_n$).

B. Single-shell asymptotic Nilsson model (SSANM)

The most deformed proton intrinsic state of ^{168}Er is obtained by placing the 18 valence protons in the first 18 ϕ_k^α states listed in Table I. These include the 10 n states with $k_\pi^n(q_k^n)=\pm\frac{1}{2}^+(7.38)$, $\pm\frac{1}{2}^+(3.85)$, $\pm\frac{3}{2}^+(3.52)$, $\pm\frac{3}{2}^+(0.24)$, and $\pm\frac{5}{2}^+(-0.19)$, and 8 a states with $k_\pi^a(q_k^a)=\pm\frac{1}{2}^-(3.18)$, $\pm\frac{3}{2}^-(2.64)$, $\pm\frac{5}{2}^-(1.54)$, and $\pm\frac{7}{2}^-(-0.09)$.

Similarly, the most deformed neutron intrinsic state of ^{168}Er is obtained by placing 12 neutrons in the n orbits with $k_\nu^n(q_k^n)=\pm\frac{1}{2}^-(9.60)$, $\pm\frac{1}{2}^-(6.17)$, $\pm\frac{3}{2}^-(5.90)$, $\pm\frac{3}{2}^-(2.70)$, $\pm\frac{1}{2}^-(2.24)$, and $\pm\frac{5}{2}^-(2.18)$, and 6 neutrons in the a orbits $k_\nu^a(q_k^a)=\pm\frac{1}{2}^+(3.69)$, $\pm\frac{3}{2}^+(3.23)$, and $\pm\frac{5}{2}^+(2.31)$. Therefore, $N_{\nu n}=12$ and $N_{\nu a}=6$. These values are slightly different from $N_{\nu n}=10$ and $N_{\nu a}=8$ obtained in the PSM from the Nilsson diagram at $\beta\approx 0.25$. The PSM values can be recovered from Table II by promoting a pair of neutrons from the $\pm\frac{1}{2}^-(2.24)$ orbits (which are the highest-lying occupied n orbits in the Nilsson diagram for ^{168}Er) to the $\pm\frac{7}{2}^+(0.92)$ orbits (which are the lowest unoccupied orbits). In this section, we will present calculations done with $N_{\nu n}=12$ and $N_{\nu a}=6$, but we have verified that the results are very similar with $N_{\nu n}=10$ and $N_{\nu a}=8$.

1. Distributions of $J_{\pi n}$ and $J_{\nu n}$

The axially symmetric intrinsic states $\mathcal{F}^{\pi n}_{K_{\pi n}}$, $\mathcal{F}^{\nu n}_{K_{\nu n}}$, and $\mathcal{F}^{n}_{K_n}$ contain even angular momenta up to $(J_{\pi n})_{\max}=14$, $(J_{\nu n})_{\max}=24$, and $(J_n)_{\max}=38$, respectively. The P_1(SSANM) distributions of $J_{\pi n}$, $J_{\nu n}$, and J_n in the corresponding intrinsic states are shown in Figs. 14(a)–14(c), in which they are compared with those obtained for the $K=0$ band of the triaxial reps in the PSM. The overall agreement is excellent.

In Figs. 14(d)–14(f), we have compared the P_1(SSANM) distributions with those obtained from the *axially symmetric* $\pi[14,0]$, $\nu[24,0]$, and [38,0] reps which contain the same set of angular momenta as the $K=0$ parts of the *triaxial* reps $\pi[10,4]$, $\nu[20,4]$, and [30,8], respectively. The agreement is not so good as before (cf. the right-hand side of Fig. 14 with the left-hand side).

2. SU_3-like distributions of J_a

The intrinsic $[\pi(h_{11/2})]^8$ and $[\nu(i_{13/2})]^8$ states contain angular momenta up to $(J_{\pi a})_{\max}=16$, and $(J_{\nu a})_{\max}=24$. The P_1(SSANM) distributions of $J_{\pi a}$, $J_{\nu a}$, and J_a in $\mathcal{F}^{\pi a}_{K_{\pi a}}$, $\mathcal{F}^{\nu a}_{K_{\nu a}}$, and $\mathcal{F}^{a}_{K_a}$ are shown in Figs. 15(a)–15(c) along with those for the SU_3 reps $\pi[16,0]$, $\nu[24,0]$, and [40,0] with same angular-momentum content. They are noticeably different. Alternately, we can match the $\overline{J}$ values in the SSANM and SU_3 as before, and the resulting distributions are shown in Figs. 14(d)–14(f). In this case, the P_1(SSANM) and $P_1(SU_3)$ distributions are very similar. The maximum angular momenta in the intrinsic state of ^{168}Er are $(J_n)_{\max}=38$, $(J_a)_{\max}=40$, and $J_{\max}=78$, according to SSANM.

C. Microscopic SU_3-symmetry model

In the simplest version of the microscopic SU_3 model [4], the intrinsic state of a nucleus is given by the Nilsson model

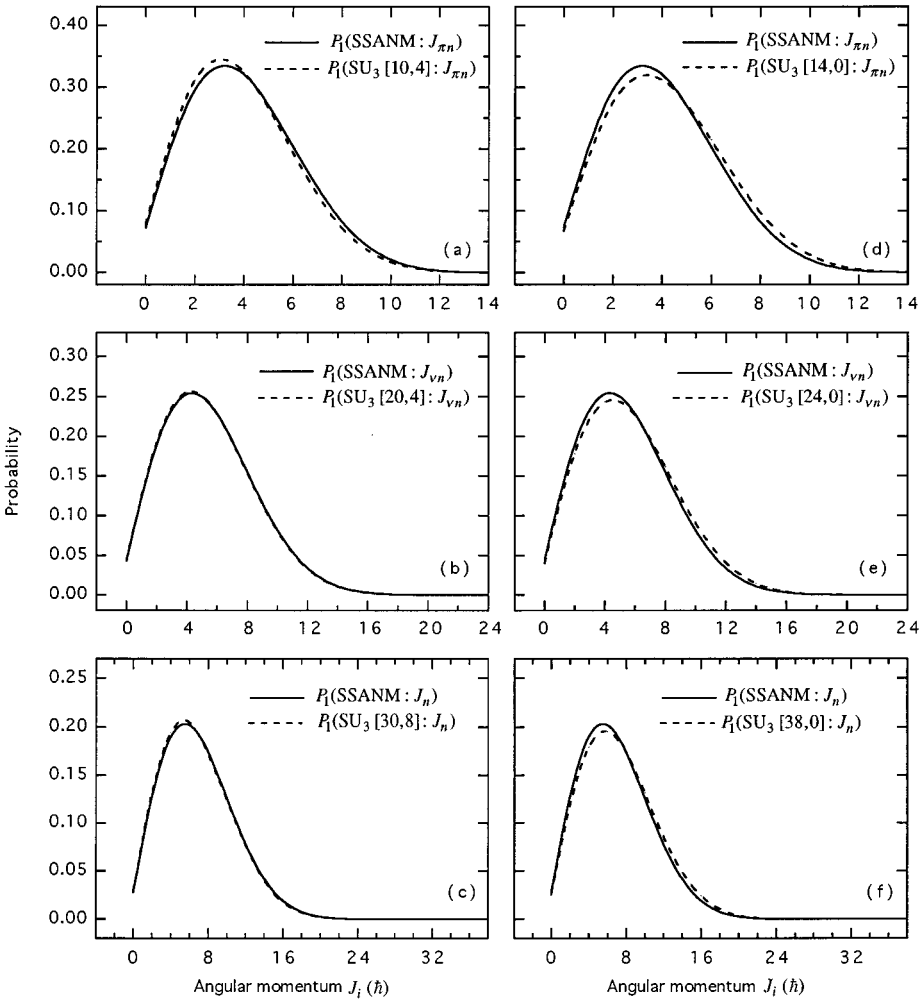

FIG. 14. P_1 distributions as a function of J_i. The abscissa is $J_{\pi n}$ in (a) and (d), J_{vn} in (b) and (e), and J_n in (c) and (f). These results are for ^{168}Er.

in which the spin-orbit interaction has been switched off. In a harmonic-oscillator potential without spin-orbit interaction, shell closures occur at neutron or proton numbers 2, 8, 20, 40, 70, 112, and 168 for the $N=0$–6 shells.

For $^{168}_{68}\mathrm{Er}_{100}$, the ''core'' for protons consists of filled shells up to $N=3$. Of the 28 valence protons in the intrinsic state, 20 occupy the most deformed sp states in the $N=4$ shell, and the remaining 8 protons occupy the intruder states of the $N=5$ shell. The asymptotically deformed states are labeled by the quantum numbers $k^{\pi}[Nn_{z'}\Lambda,q_k]$, where $k=\langle j_{z'}\rangle$, $\pi=$parity, $N=$harmonic-oscillator shell quantum number, $n_{z'}=$number of oscillator quanta along the z' axis, $\Lambda=\langle l_{z'}\rangle$, and $q_k=\langle k|q_0^2|k\rangle$ the quadrupole moment. The quantum numbers of the occupied orbits are listed in Table IV. The 10 states with $k^{\pi}=\frac{1}{2}^+$, $\frac{3}{2}^+$, $\frac{5}{2}^+$, $\frac{7}{2}^+$, and $\frac{9}{2}^+$ of the $N=4$ shell, listed in the first column of Table IV, originate from the $0g_{9/2}$ spherical state in a Nilsson diagram. The remaining 10 n states listed in the second and third columns have the same k^{π} values as the n states of protons in the 50–82 major shell used in the PSM, FDSM, and SSANM. However, their structures are significantly different. To show this, we calculate the overlap between the intrinsic states constructed from (i) the 10 SU$_3$ sp n states of the $N=4$ shell listed in the second and third columns of Table IV and (ii) the ten sp n states with the corresponding k^{π} values listed in Table I (and used in the PSM, FDSM, and SSANM). This overlap value is only 0.038. The four negative-parity states listed in the first column of Table IV are the intruder states from the $N=5$ shell with the same k^{π} values as the occupied a states used in SSANM. However, in SSANM, these intruder states are assumed to be pure $0h_{11/2}$, whereas those listed in the first column of Table IV contain admixtures from all j states belonging to the $N=5$ oscillator shell. As a result, the quadrupole moments of the a states, $q_k=10$, 7, 4, and 1 for the $k_{\pi}=\frac{1}{2}^-$, $\frac{3}{2}^-$, $\frac{5}{2}^-$, and $\frac{7}{2}^-$ states, respectively, are larger than the corresponding pure $0h_{11/2}$ values of 3.69, 3.23, 2.31, and 0.92. The overlap of the eight-proton intrinsic state constructed with (i) the $N=5$ SU$_3$ a states and (ii) the $k^{\pi}=\pm\frac{1}{2}^-$, $\pm\frac{3}{2}^-$, $\pm\frac{5}{2}^-$, and $\pm\frac{7}{2}^-$ states arising from the $0h_{11/2}$ state alone is 0.006.

We shall consider the 20 valence protons in the $N=4$ shell to be the n protons of this model. Their SU$_3$ rep is $n\pi[20,0]$ (see Table 8 of Ref. [20]). (This rep may be compared to the PSM rep $n\pi[10,4]$ for the 10 n protons in the 50–82 major shell.) The SU$_3$ rep for the eight a protons in the $N=5$ shell is $a\pi[26,4]$. Therefore, the a protons contribute up to $(J_a)_{\max}=30$, which is larger than $(J_n)_{\max}=20$ contributed by the n protons. The total SU$_3$ rep of protons is $\pi[46,4]$.

Of the 30 valence neutrons, 22 occupy the states belonging to the $N=5$ shell, and 8 occupy the intruder states belonging to the $N=6$ shell. These states are also listed in

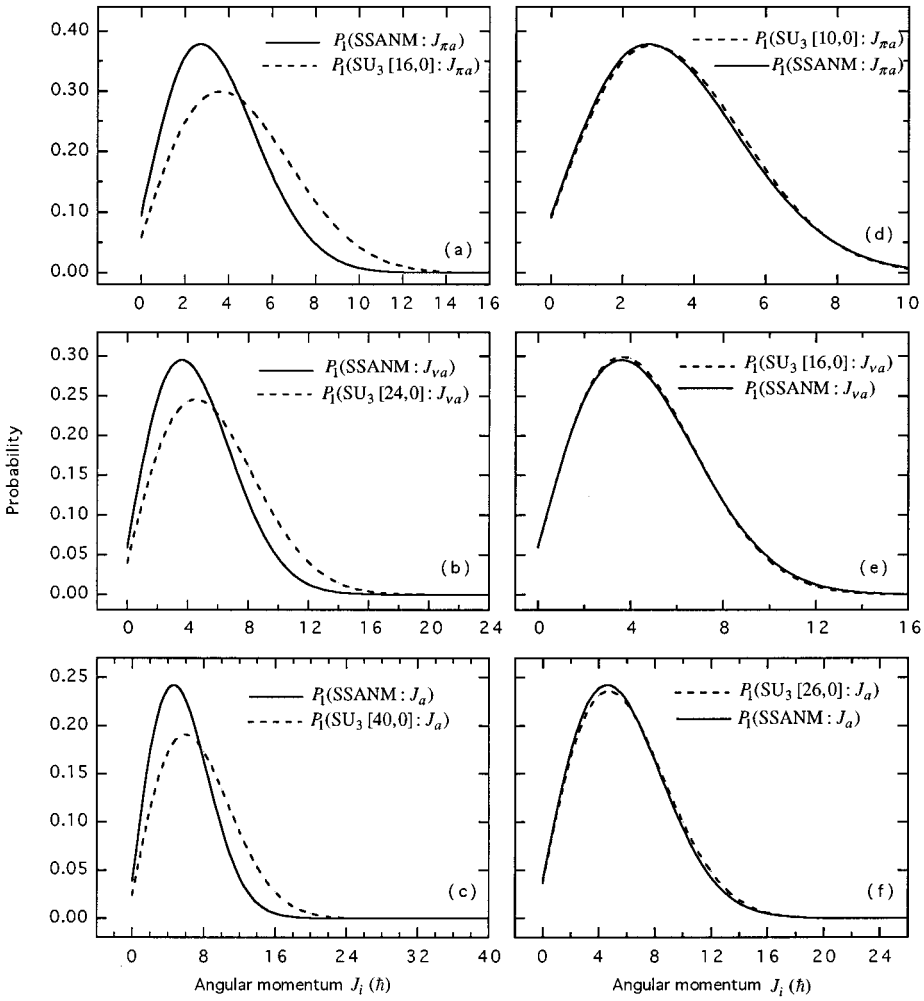

FIG. 15. P_1 distributions as a function of J_i. The abscissa is $J_{\pi a}$ in (a) and (d), J_{va} in (b) and (e), and J_a in (c) and (f). These results show SU_3-like behavior of the a nucleons in ^{168}Er also, though slightly less clearly than in the case of ^{238}U (cf. right-hand side of this figure with the same side of Fig. 9).

Table IV. The total SU_3 rep of neutrons is $\nu[66,14]$ made up of $n\nu[34,8]$ and $a\nu[32,6]$.

The total SU_3 reps for n and a nucleons in ^{168}Er are $n[54,8]$ and $a[58,10]$. Hence, according to the microscopic SU_3 model, nucleons in the a sector will contribute a little more than those in the n sector to the angular momentum of the yrast states in this nucleus.

Combining $\pi[46,4]$ with $\nu[66,14]$, the final total rep for ^{168}Er is $[112,18]$. This rep corresponds to the intrinsic state which is asymptotically deformed within the configuration space of the $N=4$ and $N=5$ oscillator shells. The intrinsic mass quadrupole moment, $(2\lambda+\mu)$, is 242. The spin-orbit interaction tends to decrease the deformation from its asymptotic value. Using the Nilsson sp states (with spin-

TABLE IV. Occupied valence asymptotic Nilsson states in ^{168}Er according to the microscopic SU_3 model. The states are labeled by $k^{\pi}[Nn_z\Lambda,q_k]$ and only those with positive k are listed. The corresponding states with negative k are also occupied.

Protons			Neutrons		
$\frac{1}{2}^+$ [440, 8]			$\frac{1}{2}^-$ [550, 10]		
$\frac{3}{2}^+$ [431, 5]	$\frac{1}{2}^+$ [431, 5]		$\frac{3}{2}^-$ [541, 7]	$\frac{1}{2}^-$ [541, 7]	
$\frac{5}{2}^+$ [422, 2]	$\frac{3}{2}^+$ [422, 2]	$\frac{1}{2}^+$ [420, 2]	$\frac{5}{2}^-$ [532, 4]	$\frac{3}{2}^-$ [532, 4]	$\frac{1}{2}^-$ [530, 4]
$\frac{7}{2}^+$ [413, -1]	$\frac{5}{2}^+$ [413, -1]	$\frac{3}{2}^+$ [411, -1]	$\frac{7}{2}^-$ [523, 1]	$\frac{5}{2}^-$ [523, 1]	$\frac{3}{2}^-$ [521, 1]
$\frac{9}{2}^+$ [404, -4]			$\frac{9}{2}^-$ [514, -2]		
			$\frac{11}{2}^-$ [505, -5]		
$\frac{1}{2}^-$ [550, 10]			$\frac{1}{2}^+$ [660, 12]		
$\frac{3}{2}^-$ [541, 7]			$\frac{3}{2}^+$ [651, 9]		
$\frac{5}{2}^-$ [532, 4]			$\frac{5}{2}^+$ [642, 6]		
$\frac{7}{2}^-$ [523, 1]			$\frac{7}{2}^+$ [633, 3]		

orbit interaction), averaged values $\langle 2\lambda+\mu\rangle$ and $\langle\mu\rangle$ have been calculated [4] as 202 and 11.5, respectively, for the ^{168}Er intrinsic state at the measured deformation. Thus, the effect of switching on the spin-orbit interaction is such that while the mass quadrupole moment is reduced by $<20\%$, the reduction in the triaxiality parameter μ is $\sim 35\%$. In the configuration space of the $N=4$ and $N=5$ shells, the yrast band of ^{168}Er extends up to $J_{\max}=130$ compared to $J_{\max}=78$ in the SSANM and $J_{\max}=38$ in the PSM.

VI. PHYSICAL ORIGINS OF ROTATIONAL STATES

While projected HF calculations (with a resonable effective interaction) do give rise to a rotationlike energy spectrum for deformed nuclei, such a spectrum is not a consequence of differences in the kinetic energy of rotation of the intrinsic state. The latter is the intuitive description of the rotational spectrum used to develop the phenomenological rigid-rotor model or the hydrodynamic model or their more satisfying microscopic extension to the Nilsson or cranked Woods-Saxon model. We follow a reasoning suggested by Khadkiker [24] to show that the energy spectrum of the states projected from an HF intrinsic state results entirely from differences in the contributions of the two-body potential energies to states of different angular momenta J.

Consider an intrinsic state $\mathcal{F}_K(\mathrm{HF})$ obtained self-consistently by an HF calculation with a Hamiltonian

$$\mathcal{H}=\sum_i (t_i+v_i)+\sum_{i<j} v_{ij} \tag{61}$$

consisting of one-body and two-body parts. The energies E_{JK} of the state Ψ^J_K projected from $|\mathcal{F}_K(\mathrm{HF})\rangle$ are given by

$$E_{JK}=\langle\Psi^J_K|\mathcal{H}|\Psi^J_K\rangle, \tag{62}$$

with Ψ^J_K given by Eq. (6a). We can write

$$E_{JK}=\frac{1}{C^*_{JK}}\frac{1}{C_{JK}}\langle\mathcal{F}_K|\mathcal{P}^J_K\mathcal{H}\mathcal{P}^J_K|\mathcal{F}_K\rangle. \tag{63}$$

Because $\mathcal{H}$ commutes with $\mathcal{P}^J_K$ and $\mathcal{P}^2=\mathcal{P}$, we get

$$E_{JK}=\frac{1}{|C_{JK}|^2}\langle\mathcal{F}_K|\mathcal{P}^J_K\mathcal{H}|\mathcal{F}_K\rangle. \tag{64}$$

This equation can be written as

$$E_{JK}=\frac{1}{|C_{JK}|^2}\sum_\Gamma \langle\mathcal{F}_K(\mathrm{HF})|\mathcal{P}^J_K|\Gamma\rangle\langle\Gamma|\mathcal{H}|\mathcal{F}_K(\mathrm{HF})\rangle, \tag{65}$$

where the states $|\Gamma\rangle$ form a complete set of states. With $\mathcal{F}_K$ as the HF state, the set $|\Gamma\rangle$ may be conveniently classified as the set of $|0p-0h\rangle$, $|1p-1h\rangle$, and $|2p-2h\rangle$ states with respect to $\mathcal{F}_K$. The term in Eq. (65) with $|\Gamma\rangle=|0p-0h\rangle$ is just the energy E_{HF} (of the state $\mathcal{F}_K$) which is independent of J. The next term with $|\Gamma\rangle=|1p-1h\rangle$ vanishes because, by definition, the Hamiltonian cannot connect the HF state to any intermediate $|1p-1h\rangle$ state. Hence, a J-dependent contribution to E_{JK} is obtained only with $|\Gamma\rangle=|2p-2h\rangle$ and only the two-body part of $\mathcal{H}$ can contribute to this term. We get

$$E_{JK}=E_{\mathrm{HF}}+\epsilon_{JK}, \tag{66}$$

where

$$\epsilon_{JK}=\frac{1}{|C_{JK}|^2}\sum_{2p-2h}\langle\mathcal{F}_K(\mathrm{HF})|\mathcal{P}^J_K|2p-2h\rangle \times\langle 2p-2h|\mathcal{H}|\mathcal{F}_K(\mathrm{HF})\rangle. \tag{67}$$

Thus the *difference* in the energies of the yrast states projected from the HF state are determined entirely by the differences in the *potential energies* of two-body interactions and not by the differences in the kinetic energy of rotation as a function of angular momentum. Although the kinetic energy part of the Hamiltonian does, by itself, contribute to the J-dependent part of the total energy of the projected state, this contribution is cancelled exactly by the contributions from the one-body potential v_i and the one-body potential extracted from the two-body interaction. Thus, the rotational spectrum of a deformed nucleus obtained in a projected HF calculation is not a consequence of the rotation of the nucleus. On the other hand, the description of the rotational band in terms of cranked HF or cranked Woods-Saxon potential model explicitly invoke rotation of the nucleus. The connection between these two descriptions of the same phenomena remains to be satisfactorily explored, although considerable progress in this direction has been made with symplectic models.

VII. SUMMARY

There is general agreement about the collective participation of protons and neutrons in generating the quadrupole collective states of a deformed nucleus. A closer examination shows that this agreement is restricted to protons and neutrons in the n sp states. Two prominent models (PSM and FDSM), specially designed to describe quadrupole collective phenomena, treat nucleons in the a sp states as spectators of the collective motion executed by nucleons in the n sp states. Other models (IBA-2, SSANM, HF, etc.) allow nucleons in states of both parities to participate actively.

We have determined the contribution of angular momenta $J_{\pi n}$ and $J_{\nu n}$ of n protons and n neutrons to the total yrast angular momentum J_n. We find that the total J_n is collectively distributed over many components of the type $|[J_{\pi n}\times J_{\nu n}]J_n\rangle$ allowed by angular momentum conservation and that these distributions, obtained for different models, are similar.

For the IBA-2 and SSANM we have, in addition, calculated (but not shown in this paper) the distribution of a yrast angular momentum J over the states $|J_\pi\rangle$ and $|J_\nu\rangle$, which contain both n and a nucleons. These distributions are similar to the one obtained for the PSM, in which only the n nucleons contribute to the total J. To bring out the contribution of the a nucleons in the IBA-2 and SSANM, we have calculated the distribution of J over the components $|[J_n\times J_a]J\rangle$. This distribution is similar to that of J over $|[J_\pi\times J_\nu]J\rangle$. This similarity shows that just as protons and neutrons contribute collectively to the yrast angular momentum, nucleons in the n and a states also do so, if permitted. In the PSM and FDSM, the a nucleons are allowed to interact with each other by a strong pairing interaction, but this

dynamic possibility is ignored for the *n* nucleons. More significantly, the *a* nucleons are denied dynamic participation in the quadrupole mean field, in which the *n* nucleons participate fully.

The PSM assumptions regarding the *a* nucleons are carried over to the symplectic extension of the model [25]. This extension does take into account explicitly the quadrupole polarization of the shell-model core resulting from interactions between valence and core nucleons, but the treatment is restricted to the *n* sector. Because core polarization arises primarily by coupling to the giant quadrupole resonance, the average contribution of the polarized core to the total angular momentum is expected to be fewer than two units. Hence, the angular-momentum content of the *n* part of the intrinsic state of a deformed nucleus, as described in the pseudosymplectic SU_3 model, should be about the same as in the PSM. Just as in the PSM, the *a* nucleons do not contribute any angular momentum to the yrast band in the implementation of the symplectic extension of the PSM reported so far [25]. The expected contribution of *a* nucleons to the total $B(E2;0_1^+\rightarrow 2_1^+)$ value can be simulated by multiplying the value obtained for the *n* nucleons with an appropriate scale factor. It would be difficult to take into account the contribution of the *a* nucleons to the total angular momentum of an yrast state by such a scaling procedure.

One of the reasons for rendering the *a* nucleons spectroscopically inert in the PSM and FDSM is that neither Elliott SU_3 symmetry nor pseudo-SU_3 symmetry exists for the j^n configuration assigned to them. The advantage of using SU_3 symmetry (for describing rotational states) is that most measured properties are well reproduced by appropriate choice of the parameters describing this symmetry, although the building blocks of SU_3 symmetry are quite different in these two models. In view of the overall agreement between measurements on the one hand and calculations involving only the *n* nucleons on the other, no strong motivation currently exists for including the effect of *a* nucleons in these models. In other words, to do so would make the calculations prohibitively large and cumbersome (if not impossible) without a comparable increase in the quality of agreement with experiment.

Projected SSANM provides a physically meaningful approach for including the contribution of the *a* nucleons to the collective rotational states while retaining the indubitable advantage of using SU_3 symmetry for the *n* nucleons. In the asymptotically deformed Nilsson intrinsic state, the *n* nucleons have good pseudo-SU_3 symmetry, but the *a* nucleons, at first sight, have no inherent underlying SU_3 symmetry. However, an important finding of this work (that partly confirms the suggestion made earlier in Ref. [11]) is that the distribution of angular momenta J_a in the *a* part of the Nilsson intrinsic state is SU_3-like. The yrast band is then generated by the quadrupole coupling of SU_3 states $|J_n\rangle$ and SU_3-like states $|J_a\rangle$ contained in the intrinsic state. An unavoidable consequence of this coupling scheme is that the probability for an yrast angular momentum *J* to be generated entirely by the *n* nucleons is very small in contrast to the coupling scheme of the PSM and FDSM in which this probability is 1. (Note that in the PSM the probability that an yrast state $|J_n\rangle$ is produced by excitation of protons alone or neutrons alone is also quite small.)

All models discussed in this paper have possibilities of improving their description of the angular-momentum structure of rotational yrast states. Unfortunately, current experiments can distinguish only between yrast states of different *J* and can give few details about how that angular momentum is generated. In spite of this drawback, it seems more reasonable that nucleons in abnormal-parity states should contribute substantially rather than not at all to the total angular momentum of collective rotation.

Recently, significant advances have occurred in the implementation of the PSM. The effect of pairing within the *n* sector has been explored in a series of papers [26]. This model is also being extended [27] to allow the *a* nucleons to participate actively in the collective dynamics. The calculations are quite complex and have not been, to our knowledge, implemented to describe the yrast bands of ^{238}U and ^{168}Er in detail. However, the results of the initial schematic calculations confirm that the *a* nucleons play an important role in the spectroscopy of deformed nuclei when they are allowed to participate in the dynamics.

ACKNOWLEDGMENTS

The current work was sponsored by the U.S. Department of Energy, under Contract No. DE-AC05-96OR22464 with Lockheed Martin Energy Research Corporation. Two of the authors (S.K. and K.H.B.) were supported in part by the Joint Institute of Heavy-Ion Research. This institute is supported by the U.S. Department of Energy, under Contract No. DE-FG05-87ER40361 with The University of Tennessee, and is operated jointly by The University of Tennessee, Vanderbilt University, and Oak Ridge National Laboratory.

APPENDIX: SOME CALCULATIONAL DETAILS

Computationally, a main problem in this paper is the calculation of the expansion coefficients $a([\lambda,\mu];J,K)$ and C_{JK} of the SU_3 and SSANM intrinsic states, respectively [see Eqs. (33) and (4)]. Knowing these coefficients, we can obtain the probabilities P_1, P_3, and P_5 from Eqs. (25), (29), and (32), respectively.

For calculating the expansion coefficients in the SU_3-based models, we use the Elliott functions $\mathcal{R}([\lambda,\mu]LKK')$ given in Eq. (36) and evaluate them using algebraic formulas [18] for SU_3 reps $[\lambda,\mu\leqslant 4]$. We switch to numerical integration when dealing with the [30,8] rep suggested in ^{168}Er (see Sec. V A). The $\mathcal{R}$ function is simply related to $a([\lambda,\mu];J,K)$ [see Eq. (35)].

In the SSANM, we construct the deformed sp orbitals ϕ_k^α from the spherical sp orbitals ψ_k^{nlj} with k being the projection $\langle j_z\rangle$. We use harmonic-oscillator wave functions as the sp spherical basis states. We make a further distinction between the *n* and *a* states. For the latter, the spherical basis consists of only one orbital; therefore, $\phi_k^1\equiv\psi_k^{nlj}$ with $c_{j,k}^1\equiv 1$. For the *n* states, we work in a single major shell. There are 4, 5, and 6 spherical sp orbitals in the 56–82, 82–126, and 126–184 shells, respectively. These orbitals are mixed by the qq interaction. The matrix elements of the sp quadrupole operator $q_0^2=\sqrt{16\pi/5}r^2Y_{20}$ between the spherical sp harmonic-oscillator states are given by [7]

$$\langle n'l'j'k|q_0^2|nljk\rangle = \frac{(j2k0|j'k)}{\sqrt{2j'+1}}\langle n'l'j'||q_0^2||nlj\rangle \tag{A1}$$

$$\langle n'l'j'||q_0^2||nlj\rangle = \sqrt{\frac{16\pi}{5}}\langle n'l'j'||r^2Y_{20}||nlj\rangle \tag{A2}$$

$$\langle n'l'j'||r^2Y_{20}||nlj\rangle = 2\sqrt{\frac{5(2j'+1)}{16\pi}}\left(j'2\frac{1}{2}0\middle|j\frac{1}{2}\right)\langle n'l'||r^2||nl\rangle \tag{A3}$$

$$\langle n'l'||r^2||nl\rangle = \sqrt{2^{l+l'-n-n'+2}\frac{(2l+2n+1)!!(2l'+2n'+1)!!}{n!n'!\pi}} \tag{A4}$$

$$\times\sum_{s=0}^{n}\sum_{s'=0}^{n'}(-2)^{s+s'}\binom{n}{s}\binom{n'}{s'}\frac{[(2s+2s'+l+l'+2+1)/2]!}{(2l+2s+1)!!(2l'+2s'+1)!!}. \tag{A5}$$

A matrix (5×5 in the case of the 82–126 shell) is built up out of these matrix elements for each possible positive value of projection k. The eigenvalues and eigenvectors of these matrices are the quadrupole moments $\langle q_k\rangle$ and the expansion coefficients $c^{\alpha}_{j,k}$ given in Tables I, II, and III.

Once the coefficients $c^{\alpha}_{j,k}$ are known, we proceed to evaluate the matrix $\langle\mathcal{F}_K|e^{-i\beta J_y}|\mathcal{F}_K\rangle$, the elements of which are given in Eq. (11). We need to pick only those $c^{\alpha}_{j,k}$ coefficients consistent with the procedure used to build the intrinsic state (see Sec. IV D 1). We employ numerical and analytical programs to compute the rotation functions $d^{J}_{KK'}(\beta)$, frequently checking numerical results with analytic calculations. In the final step, we calculate the C_{JK} coefficients by numerically integrating Eq. (14).

These calculations are done in the πn, πa, νn, and νa sectors separately. To obtain the combined C_{JK} for all nucleons in the n sector we use Eq. (30). Depending on the case of interest (all nucleons in the a sector, all protons, all neutrons, all nucleons, etc.), we invoke an expression similar to Eq. (30) for calculating the C_{JK} coefficients.

In evaluating the P_3 probabilities, we need Clebsch-Gordan coefficients of very large values of J. They are of the type $(J_1J_200|J0)$ expressible by formulas involving only multiplications and divisions. We evaluate them by summation of logarithms, thereby ensuring their respective accuracy at very large values of J.

[1] A. Bohr and B. R. Mottelson, *Nuclear Structure* (Benjamin, New York, 1969), Vols. I and II.

[2] A. de-Shalit and I. Talmi, *Nuclear Shell Theory* (Academic, New York, 1963).

[3] R. D. Ratna Raju, J. P. Draayer, and K. T. Hecht, Nucl. Phys. **A202**, 422 (1973); J. P. Draayer and K. J. Weeks, Ann. Phys. (N.Y.) **156**, 41 (1984); O. Castaños, J. P. Draayer, and Y. Leschber, *ibid.* **180**, 290 (1987); J. P. Draayer, in *International Workshop on Nuclear Structure Models*, edited by R. Bengtsson, J. Draayer, and W. Nazarewicz (World Scientific, Singapore, 1992), p. 61.

[4] M. Jarrio, J. L. Wood, and D. J. Rowe, Nucl. Phys. **A528**, 409 (1991).

[5] F. Iachello and A. Arima, *The Interacting Boson Model* (Cambridge University Press, Cambridge, England, 1987); F. Iachello and P. Van Isacker, *The Interacting Boson-Fermion Model* (Cambridge University Press, Cambridge, England, 1991).

[6] C. -L. Wu, D. H. Feng, and M. Guidry, in *Advances in Nuclear Physics*, edited by J. W. Negele and E. Vogt (Plenum, New York, 1994), Vol. 21, p. 227.

[7] C. S. Warke and M. R. Gunye, Phys. Rev. **155**, 1084 (1967); Phys. Rev. C **13**, 859 (1976).

[8] S. G. Nilsson, K. Dan. Vidensk. Selsk. Mat. Fys. Medd. **29**, No. 16 (1955).

[9] G. Ripka, in *Advances in Nuclear Physics*, edited by M. Baranger and E. Vogt (Plenum, New York, 1968), Vol. 1, p. 183.

[10] S. Pittel (private communication).

[11] K. H. Bhatt, J. C. Parikh, and J. B. McGrory, Nucl. Phys. **A224**, 301 (1974).

[12] D. Kurath and L. Picman, Nucl. Phys. **10**, 313 (1959).

[13] E. C. Halbert, J. B. McGrory, B. H. Wildenthal, and S. P. Pandya, in *Advances in Nuclear Physics*, edited by M. Baranger and E. Vogt (Plenum, New York, 1971), Vol. 4, p. 315.

[14] H. Nakada, T. Sebe, and T. Otsuka, Nucl. Phys. **A571**, 467 (1994).

[15] A. P. Zuker, J. Retamosa, A. Poves, and E. Caurier, Phys. Rev. C **52**, R1741 (1995).

[16] J. P. Elliot, Proc. R. Soc. London, Ser. A **245**, 128 (1958); **245**, 562 (1958).

[17] M. Harvey, in *Advances in Nuclear Physics*, edited by M. Baranger and E. Vogt (Plenum, New York, 1968), Vol. 1, p. 67.

[18] J. D. Vergados, Nucl. Phys. **A111**, 687 (1968).

[19] E. N. Shurshikov, Nucl. Data Sheets **53**, 601 (1988).

[20] K. H. Bhatt, S. Raman, and C. W. Nestor, Jr., Phys. Rev. C **49**, 808 (1994).

[21] B. R. Mottelson, *The Many Body Problem* (Wiley, New York, 1958).

[22] S. Raman, C. H. Malarkey, W. T. Milner, C. W. Nestor, Jr., and P. H. Stelson, At. Data Nucl. Data Tables **36**, 1 (1987).
[23] V. S. Shirley, Nucl. Data Sheets **71**, 261 (1994).
[24] S. B. Khadkiker (private communication).
[25] O. Castaños, P. O. Hess, J. P. Draayer, and P. Rochford, Nucl. Phys. **A524**, 469 (1991).
[26] D. Troltenier, C. Bahri, and J. P. Draayer, Nucl. Phys. **A586**, 53 (1995); **A589**, 75 (1975); C. Bahri, J. Escher, and J. P. Draayer, *ibid.* **A592**, 171 (1975); D. Troltenier, C. Bahri, J. Escher, and J. P. Draayer, Z. Phys. A **354**, 125 (1996).
[27] J. Escher, J. P. Draayer, and A. Faessler, Nucl. Phys. **A586**, 73 (1995); J. Escher and J. P. Draayer, Rev. Mex. Fis. **41**, Suppl. 1, 185 (1995).